A PRELIMINARY INVESTIGATION INTO THE EXTENDED LIFESPAN OF BAT SPECIES: THE RELATIONSHIP BETWEEN THE EXTRACELLULAR MATRIX PROTEIN HAS2 AND LONGEVITY

An Honors Thesis

Presented to the Honors Program of

Angelo State University

In Partial Fulfillment of the

Requirements for Highest University Honors

BACHELOR OF SCIENCE

by

AIMEE N. DENHAM

May 2015

Major: Biology

A PRELIMINARY INVESTIGATION INTO THE EXTENDED LIFESPAN OF BAT SPECIES: THE RELATIONSHIP BETWEEN THE EXTRACELLULAR MATRIX PROTEIN HAS2 AND LONGEVITY

by

AIMEE NICOLE DENHAM

APPROVED:

Dr. Loren K. Ammerman, Chair
Professor of Biology

Dr. Russell Wilke
Professor and Department Chair of Biology

May 13, 2015
Date Successfully Defended and Approved by Advisory Committee

APPROVED:

Dr. Shirley M. Eoff May 15, 2015
Director of the Honors Program

ACKNOWLEDGEMENTS

I would like to acknowledge the Angelo State University Center for Innovation and Teaching and Research for awarding me the Undergraduate Faculty Mentored Grant to fund my project. In addition, I would like to thank the Beta Beta Beta Foundation for awarding me their research grant to further fund my research project. I would not have been able to complete this project without the support and guidance from many. I would especially like to thank Dr. Loren K. Ammerman for serving as my research and thesis advisor and for sparking my interest in conducting research with bats. I could not have completed this project without her immense personal time commitment, continued support, and willingness to teach me throughout the research process. In addition, I would also like to thank Dr. Russell Wilke for serving as a member of my thesis committee and for his continued support throughout my undergraduate career. Furthermore, I would sincerely like to thank and acknowledge the Director of the Honors Program, Dr. Shirley Eoff, for allowing me the opportunity to complete an Honors undergraduate thesis, for serving on my thesis committee, and for being a constant supporter and role-model during my time at Angelo State University. I would like to extend my appreciation to Dr. Rochelle Buffenstein at the University of Texas Health Science Center for her generous donation of naked mole rat and Damaraland mole rat tissue samples. I would also like to thank Erin Adams, a graduate student at Angelo State University, for her help in netting the bats used in my research. Finally, I owe many thanks to my family and friends for their constant encouragement, support, and love.

ABSTRACT

Investigation into physiological and molecular factors influencing the extended lifespan of long-lived species significantly contributes to clinical research aimed at improving the lives of humans. Bats have a significantly longer lifespan than other mammals of similar size and have not been recorded to develop cancer. The longevity and anti-cancer properties displayed by bats are features shared by another well-studied mammal, the naked mole rat. The naked mole rat is currently the longest living rodent with a maximum lifespan of over 30 years, and the species exhibits a novel anti-cancer mechanism involving the rapid production of hyaluronan. The naked mole rat has a unique sequence of hyaluronan synthase 2 (HAS2) which rapidly produces high molecular mass hyaluronan and contributes to reduced activity of hyaluronan degrading enzymes. Known genomic sequences of several species of bats were analyzed to determine differences in amino acid sequence for the HAS2 gene. Furthermore, RNA extracted from captured bats was subjected to real-time polymerase chain reaction to measure the expression level of HAS2 in various tissues. Genomic sequence analysis revealed that the bat species examined did not have the same amino acid substitutions in HAS2 as the naked mole rat. Real-time PCR trials using multiple primers designed to be specific for the HAS2 region resulted in inconclusive data. Therefore, gene expression analysis conclusions cannot be made until successful HAS2 primers are generated to amplify the HAS2 region. Further research needs to be directed towards determining alternative methods to study the longevity and anti-cancer mechanisms bats possess.

TABLE OF CONTENTS

LIST OF FIGURES

Page

LIST OF TABLES

Page

INTRODUCTION

Life History and Characteristics of Bats

Numerous species of bats are present throughout the world, and they serve vital ecological roles in the complex web of species interactions. Bats represent the class Mammalia and the order Chiroptera which is further divided into the suborders Megachiroptera, the Old World fruit bats or flying foxes, and Microchiroptera, the wide-spread echolocating microbats. Bats are the second largest mammalian order, trailing behind rodents, with an estimated 1,116 species (Altringham, 2011). This number annually increases as new genetic evidence is revealed through the implementation and enhancement of modern molecular techniques. In addition to the immense taxonomic richness, bats also are widely dispersed around the world covering remote islands, varied climates, a wide range of latitudes, and every continent excluding the northern and southern polar regions (Altringham, 2011). Across this worldwide distribution, bats have developed remarkable characteristics that allow them to survive in diverse habitats, discover different shelter and food resources, defend against new predators, and emerge as strong competitors within the natural environment.

The diverse groups of bats share a variety of unique characteristics that highly contributes to their success and importance in ecological communities. One of the most important characteristics that bats display is the capability of flight. Bats are the only mammals that have evolved the natural ability of sustained flight via the elongation of their digits that support a flexible skin membrane (Zhang, 2013). This unique feature highly

contributes to the wide geographical distribution of bat species, and also influences some of the morphological, anatomical, and physiological changes that have occurred throughout the life history of the diverse mammalian group. The evolution of flight allows bats to shift their niche dimensions, expand their foraging area, access new food sources, and significantly reduce the chance of being faced with terrestrial predators (Adams and Pedersen, 2000). The evolution of flight has given bats enormous advantages in life and has been instrumental in the development of other unique characteristics.

With regard to diet, a majority of bats are insectivores, but some are frugivorous or feed on nectar and pollen. Others feed on organisms besides insects, including fish, frogs, and other bats, and vampire bats are known to feed on blood (Fenton, 2001). Most species of bats have developed a specialized sense of hearing known as echolocation. Echolocation is an important feature that helps bats quickly find food, avoid predators, locate roosting sites, and detect obstacles in their surrounding environment. Although bats are not the only organisms that use echolocation, this feature offers clear advantages, especially regarding feeding and roosting, for the species of bats that have evolved the characteristic. Another important feature of bats is their varying range in body size. The bumblebee bat (*Craseonycteris thonglongyai*), one of the smallest mammals, commonly weighs between 1.5-2.0 grams whereas flying foxes (*Pteropus* species) can weigh upwards of 1.0 kilogram and have a wingspan of over 1.5 meters (Altringham, 2011). Diverse size, along with the capability of flight and expansive diets, contributes to the distribution and preferred habitat of each species.

The Extended Lifespan of Bats

One of the most surprising characteristics of bats is that a large number of species have a significantly long lifespan when compared to other mammals of similar size and body mass (Podlutsky et al., 2005). The maximum lifespan of a bat is, on average, three and a half times greater than other non-flying placental mammals of similar size, and there are records of individuals from 22 species that have survived more than 20 years and five species that have survived more than 30 years in the wild (Wilkinson and South, 2002). In addition, a recaptured male Brandt's bat (*Myotis brandtii)* in Siberia was recorded to be at least 41 years old, making it the longest lived species among small mammals (Podlutsky et al., 2005). This species, and possibly other species of bats, might actually have an even longer life than previously recorded as a lack of wide-ranging research of bat longevity in the past limits documentation of maximum lifespans. Normally, the general pattern for the lifespan of mammals is that larger species live longer as compared to smaller species (Austad and Fischer, 1991). Clearly, bats are an exception to this general aging pattern when their small size and documented lifespan data are examined. In the study conducted by Podlutsky et al. (2005), the body mass and longevity record of bats, including the newly discovered 41 year old Brandt's bat, were compared to other mammal species (Figure 1). A majority of the bat species examined deviated from the normal regression line, indicating that these species display a significantly longer lifespan than expected from their small body size (Podlutsky et al., 2005). The prolonged longevity that many of the bat species display is remarkable considering the relatively low body mass of a majority of bats, especially when compared to other mammalian species.

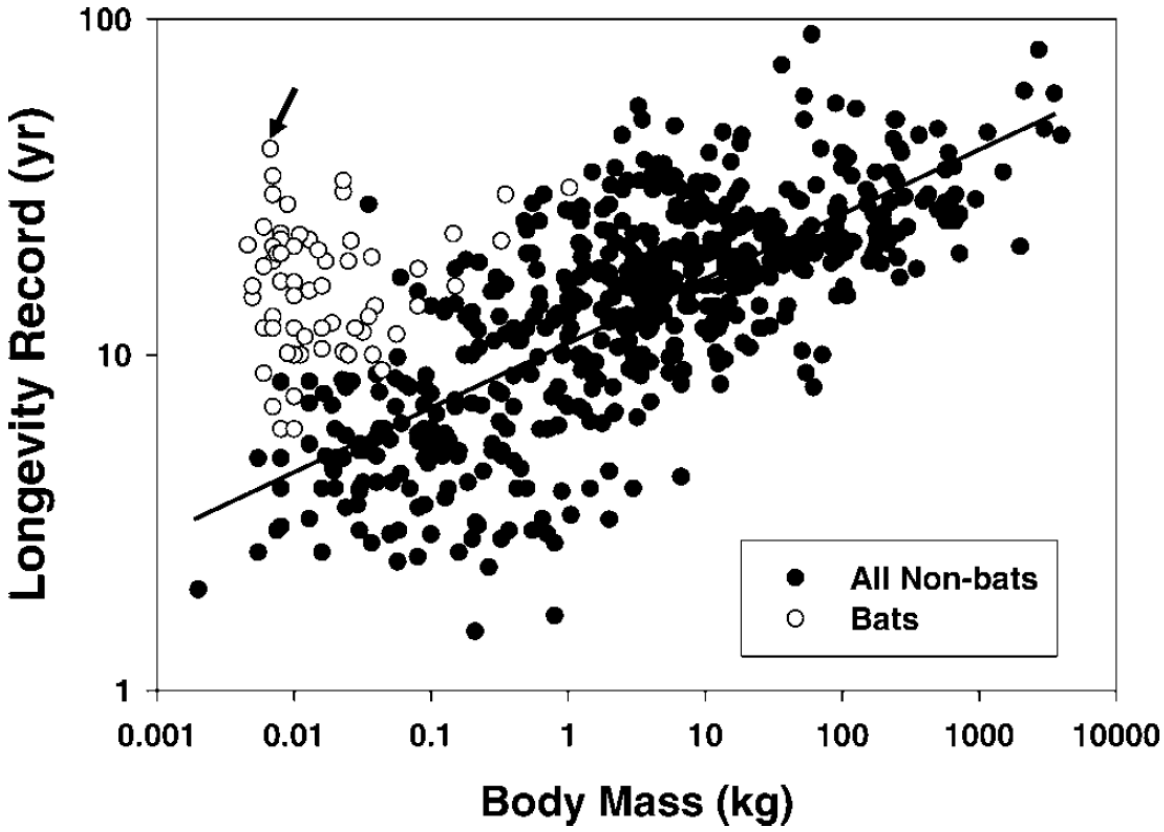

Figure 1. Longevity of bats compared with other mammal species (from Podlutsky et al., 2005). Several bat species, including the long lived Brandt's bat (arrow), have a much longer lifespan than expected given their small body size when compared to other mammals.

Behavioral and Physiological Factors Influencing the Longevity of Bats

The fact that so many species of bats display a notably extended lifespan raises questions about the factors that contribute to this unique and valuable characteristic. Without delving into the possible genetic and cellular processes that could potentially contribute to the long-life of bats, daily behavioral and physiological factors could be examined. Possible behavioral and physiological characteristics that could potentially influence the lifespan of

bats in a positive and negative way include hibernation, cave roosting, and reproduction rates.

Several of the daily actions that bats carry out are very energetically expensive, especially flight. In an effort to conserve energy, numerous species of bats undergo a physiological process known as torpor. During torpor, bats allow their body temperature to fall below the active, homeothermic level; metabolic rate, respiratory rate, oxygen consumption, and heart rate all decrease, and peripheral vasoconstriction occurs in order to maintain a warm body core temperature (Altringham, 2011). This finely controlled physiological process allows many species of bats to conserve valuable energy during times of food shortages or unfavorable weather conditions. In order to conserve energy and increase the chance of survival during cooler months when food is scarce, especially in temperate regions of the world, many species of bats undergo an extended torpor, or hibernation. In an extensive study conducted by Wilkinson and South (2002), it was found that hibernating species of bats live, on average, six years longer than species that do not hibernate. This indicates that hibernation significantly influences the lifespan of many species of bats. The way in which hibernation contributes to the extended lifespan of bats is believed to involve environmental and physiological processes. Hibernation could potentially boost the survival of bats by concealing them for long periods of time in enclosed or hard-to-reach areas. This environmental safeguard helps protect the hibernating species from dangerous extrinsic factors, such as predators or extreme weather conditions (Kunz and Fenton, 2003). On the physiological level, hibernation and periods of torpor could positively influence intrinsic age-related processes that would normally lead to somatic degradation (Kunz and Fenton, 2003). Whether the influence is from the environment or deep in the

cellular processes, it is clear that hibernation plays a minor, yet contributing, role in extending the lifespan of many species of bats.

The roosting habits of bats play a vital role in ensuring the safety and survivability of each unique species. Environmental conditions, local food and resource availability, surrounding competitors and predators, reproductive strategies, and the general morphology and physiology of bats strongly influence roost selection. (Altringham, 2011). Many obstacles influence the availability and feasibility of certain roosts, but finding the right location can positively influence the lifespan of bats. There are many types of roosts for bats, including caves, crevices, tree cavities, foliage, constructed tents, and other specialized roosts. The particular area a bat lives in strongly determines which roosting type the species will occupy. Caves serve as important roost sites for solitary bats or groups ranging up to the largest known mammalian aggregations, and many cave-dwelling bats are better protected from adverse weather conditions and deadly predators than bats roosting in more exposed areas (Kunz, 1982). Bats that occasionally roost in caves have been shown to live more than five years longer than bats that either never or always roost in caves (Wilkinson and South, 2002). Bat species that exclusively roost in caves have a higher probability of being exposed to ectoparasites or diseases that could increase chances of mortality (Lewis, 1995; Wilkinson and South, 2002), while bats that never use caves are less protected from predators or unfavorable weather conditions. More information on the incidence and transmission of ectoparasites and diseases among bat species compared to the roosting habitat needs to be conducted in order to draw more robust conclusions. However, it is clear that roosting habitat, especially cave roosting, plays an important role in the extended lifespan of many bat species.

The reproductive rate of bats significantly contributes to the displayed lifespan of bats. Female bats from species that either produce multiple pups per year or give birth multiple times per year experience shorter longevities than species that produce a single pup per year (Wilkinson and South, 2002). A higher reproductive output results in a decrease in the lifespan of the bats examined. There are several proposed reasons why reproductive rate influences the lifespan of bats. One is that there are considerable energetic demands placed on the females during fetal development and lactation after birth (Hayssen and Kunz, 1996). Pregnant females also are likely to be less agile in flight and might be more susceptible to predation (Podlutsky et al., 2005). The significant physical demands of reproduction play a vital role in influencing the longevity displayed by many species of bats.

Although the examined behavioral and physiological factors have some influence on the extended lifespan of bats, the fact that many species live longer than 20, 30, and even 40 years of age (Podlutsky et al., 2005) suggests that other highly developed cellular mechanisms are deployed in these species.

The Extended Lifespan of the Naked Mole Rat

The longevity displayed in bats is a similar characteristic seen in another mammal, the naked mole rat (*Heterocephalus glaber*). Naked mole rats belong to the order Rodentia and family Bathyergidae, also known as the blesmols or African mole rats. In addition to the naked mole rat, the Bathyergidae family includes many other mole rats from 6 genera including the Damaraland mole-rat (*Fukomys damarensis*), cape mole rat (*Georychus capensis*), silvery mole rat (*Heliophobius argenteocinereus*), Matabeleland mole rat (*Cryptomys nimrodi*), and the cape dune mole rat (*Bathyergus suillus*). The naked mole rat is

a colonial species found in sub-Saharan Africa that lives in large, complex systems of underground burrows. Naked mole rats have a smooth, highly elastic skin membrane, a blunt head with large incisor teeth for digging and foraging, and several adaptations to living in hypoxic conditions (Bennett and Faulkes, 2000). The naked mole rat's unique appearance and several physiological adaptations allow the organism to successfully survive in underground tunnels.

Naked mole rats are currently the longest living rodents with a maximum documented lifespan of 32 years which is five times longer than expected based on body size and over ten times longer than a mouse (Buffenstein, 2008; Edrey et al., 2011). In comparison, the house mouse has a maximum lifespan of four years and the Damaraland mole rat has a maximum lifespan of 20 years (Fang et al., 2014). In comparing the body mass and maximum lifespan, naked mole rats deviated from the normal regression line which indicates that this species displays a significantly longer lifespan than expected for their small body size (Healy et al., 2014). This feature is comparable with the body mass and maximum lifespan features of bat species previously examined. Naked mole rats incredibly do not experience some of the common characteristics associated with the process of aging. During their long lifespan, naked mole rats maintain their body composition, bone density, and metabolic rate, and they display remarkable genomic and proteomic integrity (Lewis et al., 2013). In addition, a proposed and heavily studied contributing factor to the extended lifespan displayed by the species is their ability to resist cancer. Clearly, complex physiological mechanisms present in this species heavily contribute to their senescent properties and long lifespan.

Recently, naked mole rats have been discovered to display a novel anti-cancer mechanism involving the rapid production of a modified form of hyaluronan (HA) caused by

two unique serine substitutions in hyaluronan synthase 2 (HAS2), one of the HA synthesizing enzymes (Tian et al., 2013). HA is a high-molecular-mass polysaccharide that serves as an integral component within the extracellular matrix and various tissues and organ systems. Physiologically, hyaluronan is involved in inflammation and wound repair, mitotic cell division, and cell migration (Fraser et al., 1997; Chen and Abatangelo, 1999; Kothapalli et al., 2007; Tolg et al., 2014). Collectively, these cellular processes are components associated with many physiological processes as well as the development and progression of certain cancers. The secretion of high-molecular-mass HA (HMM-HA), the modified form of HA, within naked mole rats is an adaptation that contributes to the loose, stretchy skin membrane needed for life in small underground tunnels (Tian et al., 2013). Coincidentally, the HMM-HA that contributes to this unique life characteristic now serves as the primary driving molecule behind the displayed anti-cancer and longevity properties of the species.

The anti-cancer mechanism in naked mole rats involves early contact inhibition (ECI), which is a process of arresting cell growth when cells come in contact with extracellular matrix components or other cells (Tian et al., 2013). Previously, naked mole rat cells were found to display hypersensitivity to contact inhibition by activation of p53 and pRb tumor suppressor pathways (Seluanov et al., 2009). A study conducted by Tian et al. (2013) found that the HMM-HA present in naked mole rats also triggered ECI through the CD44 receptor. Both of these ECI mechanisms play a significant role in facilitating the cancer resistance and subsequently the long-life of naked mole rats. In addition to ECI, it also was found that rapid accumulation of HMM-HA synthesized by the unique HAS2 enzyme contributed to reduced activity of hyaluronidase (HAase) activity, leading to even greater accumulation of HMM-HA within the extracellular matrix (Tian et al., 2013).

Furthermore, HMM-HA has been shown to induce inhibitors of cyclin dependent kinase 4 (INK4), a tumor suppressor protein, which leads to cell cycle arrest within naked mole rat cells (Tian et al., 2015). The rapid synthesis, reduced degradation, and ECI signaling and tumor suppressor pathways that HMM-HA is readily involved in all contribute to the remarkable cancer resistance and extended lifespan displayed by naked mole rats.

Significance of Studying Aging and Cancer

The study of aging represents a rapidly emerging field within the scientific community, especially with regard to investigating life extension and age-related diseases. The process of aging is influenced by numerous factors and is regularly characterized by an increase in genomic instability, an accumulation of oxidative stress, increases in pathological disorders, and an increase in mortality (Lewis et al., 2013). Organisms that display extended lifespans, like bats and naked mole rats, provide molecular clues in regard to the biological and physiological processes that influence aging. These long-lived species serve as unique models of aging, and understanding the life history variables and physiological mechanisms that contribute to their extended lifespan could potentially be applied to humans.

Uncovering the reasons why long-lived species have extended lifespans and no incidences of cancer could significantly aid in human research. The naked mole rat is one particular organism that shows great potential as a unique model in the understanding and development of cancer prevention and treatment strategies for humans. There has been extensive research on the importance of hyaluronan in the human body, especially with regard to cellular interactions and cancer. Hyaluronan occurs universally throughout the body, especially in the skin, connective tissue, synovial fluid, vitreous body of the eye, and

intervertebral disks, and is a major component in fetal structures and development (Karbownik and Nowak, 2013). Due to the wide distribution of hyaluronan within the body, there are a high number of medical applications, particularly in fields such as ophthalmology, dermatology, rheumatology, gynecology, otolaryngology, and oncology (Karbownik and Nowak, 2013). The role of hyaluronan and hyaluronan-interacting molecules currently is being investigated to determine novel anti-cancer mechanisms that have the potential to significantly impact the field of oncology.

One important feature of hyaluronan is the variety of sizes that the molecule displays. Two different common forms of hyaluronan within the body: high molecular mass hyaluronan, or HMM-HA, which is then readily broken down into low molecular mass hyaluronan, or LMM-HA. This difference in the form of hyaluronan is significant with regard to the function within the body. HMM-HA is involved in early contact inhibition due to hypersensitivity to high cell density levels (Seluanov et al., 2009; Tian et al., 2013), arrest of mitogenic signaling within the cell cycle due to interaction with the CD44 receptor (Kothapalli et al., 2007), and many anti-inflammatory properties (Pure and Assoian, 2009). Each of these important effects of HMM-HA can contribute to anti-cancer mechanisms within the body. In contrast, LMM-HA is associated with promoting cell cycle progression due to interaction with the CD44 receptor (Kothapalli et al., 2008) and also stimulates inflammation and cellular proliferation (Pure and Assoian, 2009). These factors support the formation of tumors and the development of cancer within the body. Hyaluronan size has a great influence on cellular signaling pathways which results in different biological and physiological outcomes. Clearly, the synthesis and degradation patterns of hyaluronan molecules are very important in the development of cancer. Therefore, discovering ways to

modify the synthesis, degradation, or interactions that hyaluronan is involved in within the body could lead to significant clinical applications in cancer prevention and treatment.

As shown in the naked mole rat, HMM-HA plays a significant role in mediating cancer resistance and the extended lifespan of the species. Malignant transformation and anchorage-independent growth occurred when HAS2 was knocked out, HAase activity was overexpressed, and the CD44 receptor was blocked (Tian et al., 2013). Therefore, interfering with the hyaluronan synthesizing enzyme, hyaluronan degrading enzyme, and the tumor suppressor pathway receptor all play a key role in anti-tumor development pathways in naked mole rats. Understanding the connection between the molecular mechanisms and physiological responses occurring within naked mole rats allows targeted research to begin with the hopes of clinical applications. Discovering ways to manipulate the production, degradation, and HA-triggered pathways as shown in the naked mole rat within the human body could potentially uncover new ways to prevent or stop the development of cancer. This will subsequently help extend the lifespan and improve the overall health of many individuals.

Objective

Bats and naked mole rats share numerous features, most notably the extended lifespan, small body mass and size, and highly elastic skin membrane. For both bats and naked mole rats, the development of elastic skin membranes needed for flight and life in underground tunnels occurred through advanced evolutionary processes. The unique sequence of HAS2 and reduced activity of HA-degrading enzymes contributes to the highly elastic skin membrane and the extended lifespan of the species (Tian et al., 2013), but

extensive research into this particular molecular mechanism contributing to the long lifespan of bats has not been studied. After examining the evolutionary history and shared features of bats and naked mole rats, it was hypothesized that bats have the same unique amino acid substitutions for HAS2 as found in the naked mole rat. Alternatively, it was hypothesized that bats would have high expression levels of HAS2 in their tissue, especially in the wing membranes. It is clear that bats and naked mole rats serve as unique models of aging and longevity, but research into the specific mechanisms contributing to their long life needs to be further examined. Examination into this specific mechanism will provide valuable information regarding the extended lifespan of many bat species and will further contribute to the body of scientific research regarding longevity studies.

METHODS

Protein Sequence Analysis

HAS2 protein sequences for various mammals, including three mole rat species, four bat species, human, house mouse, and other common mammals, were retrieved from GenBank in January 2015. The mole rat species included the naked mole rat (*Heterocephalus glaber*), Damaraland mole rat (*Fukomys damarensis*), and the blind mole rat (*Nannospalax galili*). The bat species included the big brown bat (*Eptesicus fuscus*), Brandt's Bat (*Myotis brandtii*), little brown bat (*Myotis lucifugus*), and the black flying fox (*Pteropus alecto*). The protein sequences were aligned and analyzed using *MEGA* version 6 in order to find unique polymorphisms that each species could potentially exhibit (Tamura et al., 2013). This step determined if the bat species or any other mammal examined displayed the same unique sequence of HAS2 that is present in naked mole rats, as described by Tian et al. (2013).

Tissue Collection

In the fall of 2014, two species of bats (*Nycticeius humeralis,* evening bat; *Lasiurus cinereus*, hoary bat) were collected from the Head of the River Ranch located in Christoval, Texas, and one species (*Myotis velifer*, cave myotis) was collected from the Foster Road bridge in San Angelo, Texas. Tissue samples from the liver, kidney, heart, and wing membrane were collected and immediately stored in RNAlater RNA Stabilization Reagent (Qiagen, Valencia, CA) to preserve the tissue. After tissue collection, the bats and frozen tissue samples were deposited into the Angelo State Natural History Collections for future research (*N. humeralis* – ASK 10733, *L. cinereus* – ASK 10734, and *M. velifer* – ASK

10737). Bats were collected under Texas Parks and Wildlife Scientific Research permit #SPR-0994-703.

Mole rat tissue samples, including *Heterocephalus glaber* (naked mole rat) and *Fukomys damarensis* (Damaraland mole rat), were donated by the Barshop Institute for Longevity and Aging Studies lab at the University of Texas Health Science Center at San Antonio. Liver, kidney, heart, and skin tissue samples from two naked mole rats and two Damaraland mole rats were collected and stored in RNAlater RNA Stabilization Reagent.

A house mouse (*Mus musculus)* retrieved from Angelo State University's mouse colony served as a comparison model in the study. Liver, kidney, heart, skin, and ear tissue samples were collected and stored in RNAlater RNA Stabilization Reagent.

Primer Design

Reference genes, including β-actin (ACTB) and glyceraldehyde 3-phosphate dehydrogenase (GAPDH), and multiple primers for HAS2 were designed or retrieved from several sources (Table 1). New HAS2 primers were designed and created specifically with the intention of working with the collected mouse, mole rats, and bat species. Sequences for the HAS2 gene from the available bat, mole rat, and mouse species were retrieved from GenBank. The primer design tool from the database was utilized in order to find conserved regions from each of the desired species to be used as primers. The primers created were between 19 and 20 base pairs in length. Once the specific primer pairs were found, each primer was analyzed in OligoAnalyzer 3.1 (Integrated DNA Technologies, Coralville, IA). This program reveals important primer features, including the base content, estimated

melting temperature, self-dimer probability, hairpin likelihood, and other characteristics. All primers were purchased from AlphaDNA (Quebec, Canada).

Table 1. HAS2 Primers designed or retrieved from previous studies

Primer Name	**DNA Sequence (5'- 3')**	**Source**
HAS2-Forward	GAAAAGGGTCCTGGTGAGACGGATGAG	Tian et al., 2013
HAS2-Reverse	TTCACCATCTCCACAGATGAGGCAGG	Tian et al., 2013
ACTB-Forward	GAAATCGTGCGCGACATCAA	Designed
ACTB-Reverse	ATGGGACCGTTAGCACAAG	Designed
GAPDH-Forward	GACCACAGTCCATGCCATCA	Redfern et al., 2011
GAPDH-Reverse	GTCAAAGGTGGAGGAGTGGG	Designed
HAS2(1)-Forward	GAAGACCCCATGGTTGGAGG	Designed
HAS2(1)-Reverse	TTCCGCCTGCCACACTTATT	Designed
HAS2(2)-Forward	AGAGTGCTGAGTCTGGGCTA	Designed
HAS2(2)-Reverse	AAGAGCTGGATTACCGTGGC	Designed
HAS2(3)-Forward	AGAGCACTGGGACGAAGTGT	Chun-E et al., 2015
HAS2(3)-Reverse	ATGCACTGAACACACCCAAA	Chun-E et al., 2015
HAS2(4)-Forward	TGGGCGAGAAATTGAGTGTT	Zhu et al., 2014
HAS2(4)-Reverse	GGTCTCCACATTCCTGCCA	Zhu et al., 2014
HAS2(5)-Forward	CAGAGGGCCAGATGAACACT	Zhu et al., 2014
HAS2(5)-Reverse	GGATCTGCTTCACTGCCTCT	Zhu et al., 2014
HAS2(6)-Forward	CTGTGAAAAGGCTGACCTAC	Sugiyama et al., 1998
HAS2(6)-Reverse	TCAGTAAGGCACTTGGACCG	Sugiyama et al., 1998
HAS2(7)-Forward	GCAGGCGGAAGAAGGGACAAC	Jenkins et al., 2004
HAS2(7)-Reverse	TCAGGCGGATGCACAGTAAGGA	Jenkins et al., 2004

RNA Isolation and cDNA Synthesis

RNA isolation of the tissue samples stored in RNAlater was completed using the RNAqueous-4PCR Kit (Ambion Life Technologies, Grand Island, NY) following the manufacturer's protocol. There were two elutions of 50 µl completed for each sample isolated. cDNA synthesis was completed using the iScript cDNA Synthesis Kit (Bio-Rad, Hercules, CA) following the manufacturer's protocol. The cDNA generated served as the starting template that was used in determining the level of gene expression of HAS2 within each of the tissue samples examined. The concentration and purity ratio of the isolated RNA and synthesized cDNA was measured using the NanoDrop Lite Spectrophotometer (Thermo Scientific, Waltham, MA) following the manufacturer's protocol.

RNA isolation and cDNA synthesis began with the liver and wing membrane tissue samples from each of the three bat species since mouse and mole rat tissue samples were collected later in the study. RNA isolation and cDNA synthesis of kidney and heart tissue samples from each of the three bat species along with mouse liver, skin, and ear tissue samples were collected following several trial runs with the bat liver and wing membrane tissue samples.

Real-Time Polymerase Chain Reaction (PCR) and Gene Expression Analysis

The generated cDNA was subjected to real-time PCR using a CFX Connect Real-Time PCR Detection System machine (Bio-Rad, Hercules, CA). Real-time PCR was completed following the SsoAdvanced Universal SYBR Green Supermix protocol developed by Bio-Rad. The quantification data, melting curve, and relative quantity gene expression was analyzed using the Bio-Rad CFX Manager Program. A gene study was created using the

Bio-Rad CFX Manager Program which combined multiple trials into a comprehensive gene expression analysis. Real-time PCR cycling conditions began with a denaturation step at 95ºC for 30 seconds, and then the samples were cycled 40 times at 95ºC for 15 seconds and at 60ºC for 1 minute. The final step included a melting curve that occurred from 65.0ºC to 95ºC at 0.5ºC increments for 5 seconds per step. The addition of a melt curve was important in analyzing the dissociation characteristics of the products and was used to reveal nonspecific products by examining the number of melt peaks. During some of the trials, the annealing temperature was decreased to 58ºC or increased to 62ºC in an effort to improve the quantification results. In addition, the starting cDNA template was decreased from 1.0 µl to 0.5 µl or increased from 1.0 µl to 1.5 µl in an effort to improve the quantification results. The products following real-time PCR were separated by electrophoresis on a 1.0% agarose NaB gel with ethidium bromide and visualized on a UV transilluminator in order to ensure that proper amplification was occurring.

Conventional PCR of cDNA

Following failed trials of real-time PCR, conventional PCR of cDNA was completed with five newly ordered primers in order to determine if any of the primers would produce positive results. The cDNA generated from the *N. humeralis* liver and wing membrane tissue samples was used to test each of the primers. The profile for PCR began with a denaturation step at 94ºC for 2 minutes. The samples were then cycled 35 times at 94ºC for 30 seconds, 59ºC for 1 minute, and 72ºC for 1 minute. The final step was completed at 72ºC for 5 minutes. Products were separated on a 1% agarose gel by electrophoresis.

DNA Extraction and Conventional PCR

Following unsuccessful real-time PCR trials, DNA was extracted from mouse, naked mole rat, Damaraland mole rat, hoary bat, and cave myotis liver tissue samples using the DNeasy Blood and Tissue Kit (Qiagen) following the manufacturer's protocol. The concentration and purity ratio of the extracted DNA was determined using the NanoDrop Lite Spectrophotometer (Thermo Scientific). All primers, including the reference genes ACTB and GAPDH, were used in a conventional PCR run using the extracted DNA as the template to determine which primers exhibited positive or negative amplification of HAS2. The profile for PCR consisted of a denaturation step at 94ºC for 2 minutes, and then the samples were cycled 35 times at 94ºC for 30 seconds, 59ºC for 1 minute, and 72ºC for 1 minute. The final step was at 72ºC for 5 minutes. Products were separated on a 1% agarose gel by electrophoresis.

RESULTS

Protein Sequence Analysis

The sequences from the 4 bat species examined from Genbank did not have the same unique amino acid sequence in HAS2 as the naked mole rat (Figure 2). The amino acid residues in the bats were identical to those of other mammals, except the Damaraland mole rat (*F. damarensis*) which contained the same unique sequence as the naked mole rat. The naked mole rat and Damaraland mole rat display unique amino acid changes from asparagine (N) to serine (S) residues at site 301 in the HAS2 protein sequence.

Name	Common Name	Accession #	L	S	S	K	W	Y	S	Q
Heterocephalus glaber	Naked Mole Rat	NP_005319.1	·	·	·	·	·	·	·	·
Fukomys damarensis	Damaraland Mole Rat	XP_010633719.1	·	·	N	·	·	·	·	·
Nannospalax galili	Blind Mole Rat	XP_008836208.1	·	·	N	·	·	·	N	·
Homo sapiens	Human	NP_005319.1	·	·	N	·	·	·	N	·
Mus musculus	House Mouse	NP_032242.3	·	·	N	·	·	·	N	·
Eptesicus fuscus	Big Brown Bat	XP_008141578.1	·	·	N	·	·	·	N	·
Myotis brandtii	Brandt's Bat	XP_005885929.1	·	·	N	·	·	·	N	·
Myotis lucifugus	Little Brown Bat	XP_006085313.1	·	·	N	·	·	·	N	·
Pteropus Alecto	Black Flying Fox	XP_006916646.1	·	·	N	·	·	·	N	·
Rattus norvegicus	Brown Rat	NP_037285.1	·	·	N	·	·	·	N	·
Oryctolagus cuniculus	European Rabbit	NP_001075479.1	·	·	N	·	·	·	N	·
Pan troglodytes	Chimpanzee	XP_528222.2	·	·	N	·	·	·	N	·
Callithrix jacchus	Common Marmoset	XP_002759314.1	·	·	N	·	·	·	N	·
Canis lupus familiaris	Domestic Dog	XP_539153.1	·	·	N	·	·	·	N	·
Ailuropoda melanoleuca	Giant Panda	XP_011233905.1	·	·	N	·	·	·	N	·
Bos taurus	Cow	NP_776504.1	·	·	N	·	·	·	N	·
Sus scrofa	Wild boar	NP_999218.1	·	·	N	·	·	·	N	·
Ornithorhynchus anatinus	Platypus	XP_001505240.1	·	·	N	·	·	·	N	·
		Site Number:			178				301	

Figure 2. Variation in amino acid sequence alignment of 4 bat species, 3 mole rat species, and several mammals included in Tian et al. (2013). Site number 301 displays the amino acid change from asparagine (N) to serine (S) that is unique to the naked mole rat and Damaraland mole rat. The naked mole rat's amino acid sequence is displayed across the top. Dots represent amino acid residues that are identical to the sequence at the top. Sequences were retrieved and aligned January 2015.

RNA Isolation and cDNA Synthesis Trial 1

The amount of RNA recovered from the liver and wing membrane tissue samples from each of the three bat species resulted in a higher concentration of RNA in the first elution as compared to the second elution (Table 2). In addition, the concentration of RNA extracted from each of the liver tissue samples for the three bat species was higher than the wing membrane tissue samples. The purity ratio of RNA for each of the tissue samples examined was between 1.79 and 2.20. The desired purity ratio range for RNA is near 2.0 to 2.1, so some of the values are outside the target range. Only the first elution from the RNA isolation was used in the cDNA synthesis. The adjusted concentration of cDNA (Table 3) was higher in each of the liver tissue samples as compared to the wing membrane tissue samples. The purity ratio of cDNA for each of the tissue samples examined was between 1.83 and 1.84, which falls near the desired range of 1.80.

Table 2. RNA quality and concentration of tissue samples from each bat species examined (*N. humeralis* – ASK 10733, *L. cinereus* – ASK 10734, and *M. velifer* – ASK 10737).

Sample	Elution #	Purity Ratio	Concentration (µg/ml)
N. humeralis Liver	1	1.85	31.2
N. humeralis Liver	2	1.86	10.9
N. humeralis Wing Membrane	1	1.95	22.4
N. humeralis Wing Membrane	2	1.86	9.8
L. cinereus Liver	1	2.20	40.1
L. cinereus Liver	2	2.19	25.5
L. cinereus Wing Membrane	1	1.99	14.9
L. cinereus Wing Membrane	2	1.97	7.6
M. velifer Liver	1	2.12	20.0
M. velifer Liver	2	1.79	3.7
M. velifer Wing Membrane	1	1.92	13.9
M. velifer Wing Membrane	2	1.90	7.8

Table 3. Quality and concentration of cDNA generated from tissue samples from each bat species examined (*N. humeralis* – ASK 10733, *L. cinereus* – ASK 10734, and *M. velifer* – ASK 10737).

Sample	Elution #	Purity Ratio	Concentration (µg/ml)	Adjusted Concentration (µg/ml)**
Blank* Negative Control	N/A	1.83	986.1	N/A
N. humeralis Liver	1	1.84	1136.6	150.5
N. humeralis Wing Membrane	1	1.83	1103.2	117.1
L. cinereus Liver	1	1.84	1199.5	213.4
L. cinereus Wing Membrane	1	1.83	1052.2	66.1
M. velifer Liver	1	1.83	1090.2	104.1
M. velifer Wing Membrane	1	1.83	1037.2	51.1

*Blank contained the 5X iScript Reaction Mix, iScript Reverse Transcriptase, and the Nuclease Free Water used during cDNA synthesis
**Adjusted Concentration is the sample concentration subtracted from the blank measurement

Real-Time PCR

Numerous real-time PCR experiments were performed with various primer sets, starting cDNA concentrations, and cycling profiles. Selected results from several notable and crucial trials are discussed in the following real-time PCR trial sections.

Real-Time PCR Trial 1

The cDNA generated from *N. humeralis* liver and wing membrane tissue samples was used for the first trial of real-time PCR using the HAS2, GAPDH, and ACTB primers. Quantification data revealed that each sample successfully showed amplification without any of the negative controls amplifying (Figure 3). The reference gene GAPDH amplified first at cycle 24 for the wing membrane tissue sample and 27 for the liver tissue sample, followed by HAS2 at cycle 31 for the wing membrane tissue sample and 32 for the liver tissue sample. The reference gene ACTB amplified last at cycle 35 for both the wing membrane tissue and liver tissue samples.

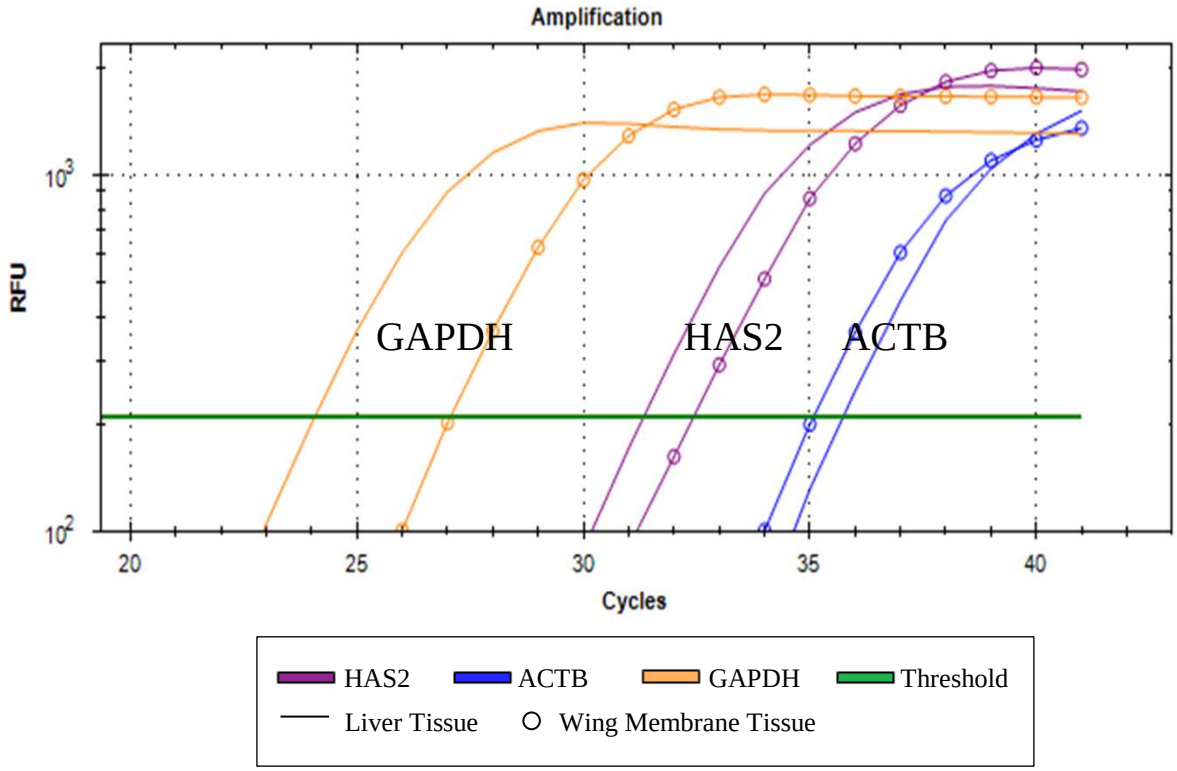

Figure 3. Real-time PCR amplification curve of *N. humeralis* liver and wing membrane tissue samples with HAS2 primer set. All samples exhibited successful amplification. Primers include HAS2 (purple), GAPDH (orange), and ACTB (blue). Number of cycles is plotted with the relative fluorescence unit (RFU) in order to quantify the amplified cDNA. Solid lines represent liver tissue samples and lines with circles represent wing membrane tissue samples.

Melt peak analysis (Figure 4) revealed two strong peaks at 86.5ºC, the expected product melting temperature, for GAPDH. The peaks for ACTB were at the melting temperature 76.5ºC and 77.0ºC. The first peak for HAS2 with the liver tissue sample showed two peaks occurring at 82.5ºC and 88.0ºC, indicating the presence of an unspecific product. The second peak for HAS2 with the wing membrane tissue sample showed one peak at 88.0ºC, the expected product melting temperature.

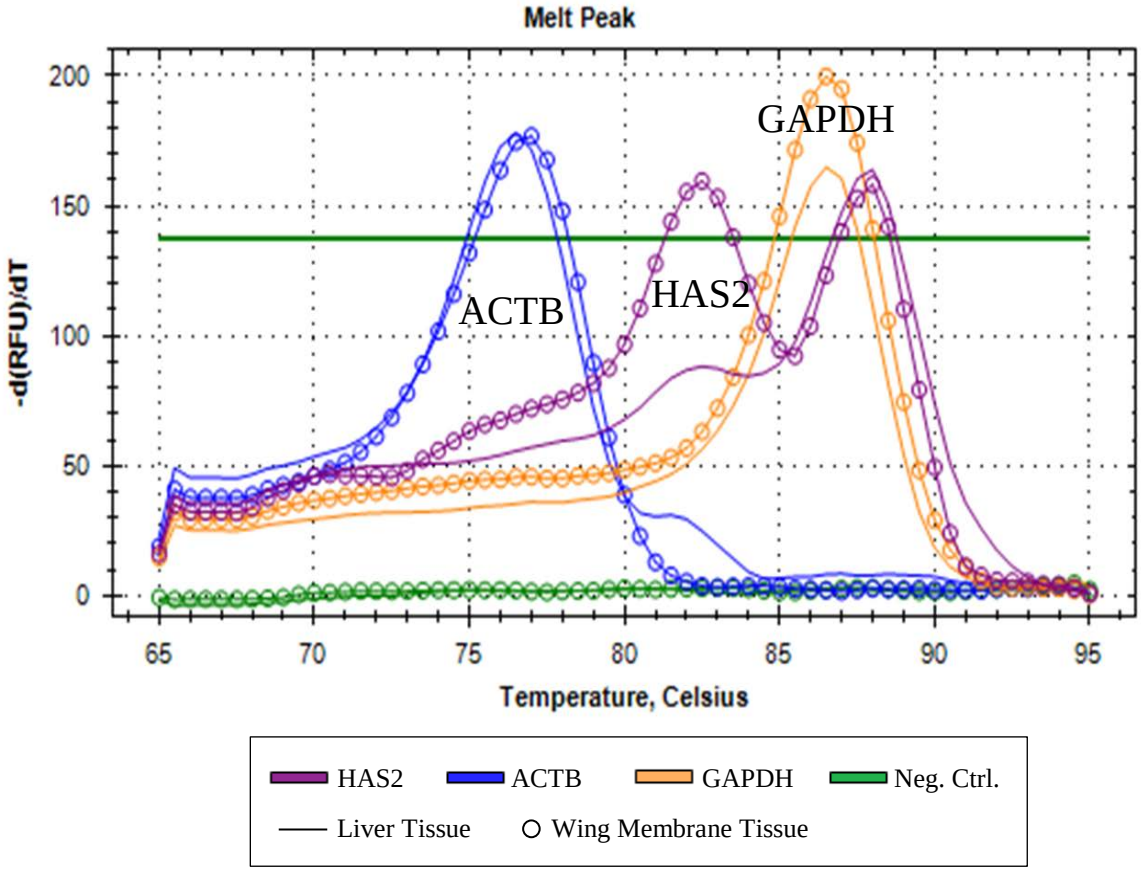

Figure 4. Real-time PCR melt peak analysis of *N. humeralis* liver and wing membrane tissue samples. Primers include HAS2 (purple), GAPDH (orange), and ACTB (blue). HAS2 produces two peaks, indicating the presence of unspecific product. Solid lines represent liver tissue samples and lines with circles represent wing membrane tissue samples. Negative control samples are green.

Relative quantity (ΔCq) gene expression analysis showed that HAS2 was expressed more in wing membrane tissue as compared to the liver tissue, but it was not overexpressed relative to the reference genes used (Figure 5). Relative quantity gene expression displays the gene concentration relative to other samples in the experiment.

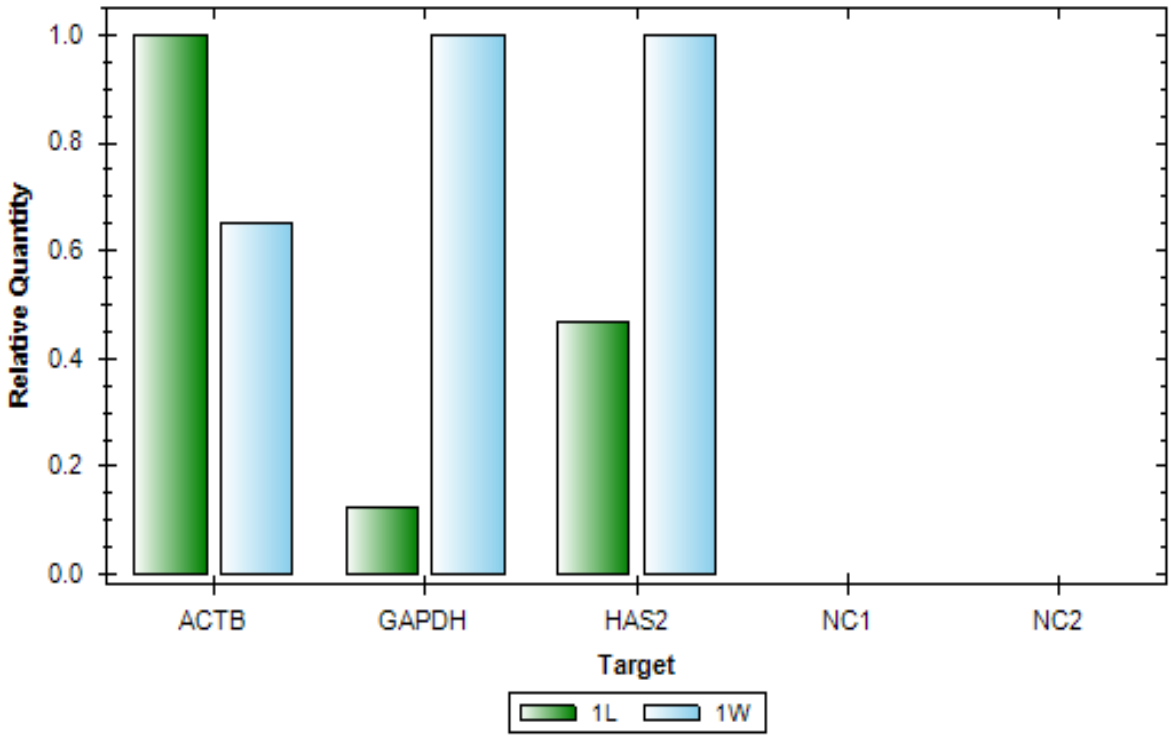

Figure 5. Relative quantity (ΔCq) gene expression of *N. humeralis* (1) liver (L) and wing membrane (W) tissue samples.

Electrophoresis analysis using a 1.0% agarose gel resulted in faint banding for HAS2 at around 350 base pairs, a strong band for GAPDH at around 400 base pairs, and no banding for ACTB (Figure 6).

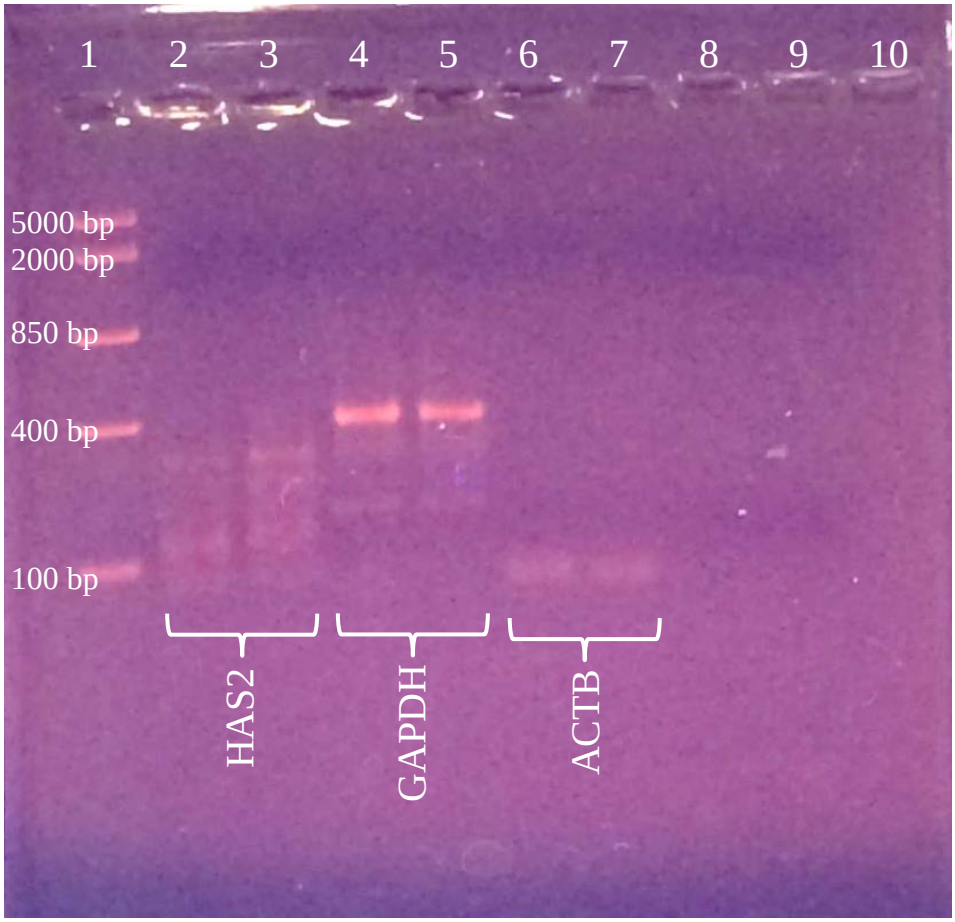

Figure 6. Electrophoresis analysis of *N. humeralis* liver and wing membrane tissue samples. Samples include HAS2 liver and wing membrane tissue (lanes 2 and 3), GAPDH liver and wing membrane tissue (lanes 4 and 5), and ACTB liver and wing membrane tissue (lanes 6 and 7). HAS2 showed slight banding at around 350 base pairs, and GAPDH showed strong banding at around 400 base pairs. No banding was associated for ACTB. Lane 1 contains the mid range DNA ladder.

Real-Time PCR Trial 2

The cDNA generated from *N. humeralis, L. cinereus, and M. velifer* liver and wing membrane tissue samples were subjected to real-time PCR using HAS2, GAPDH, and ACTB primers. Quantification data revealed that each sample successfully showed amplification without any of the negative controls amplifying (Figure 7). GAPDH amplified first between cycles 24 and 29, followed by HAS2 between cycles 32 and 34. ACTB amplified last between cycles 32 and 37.

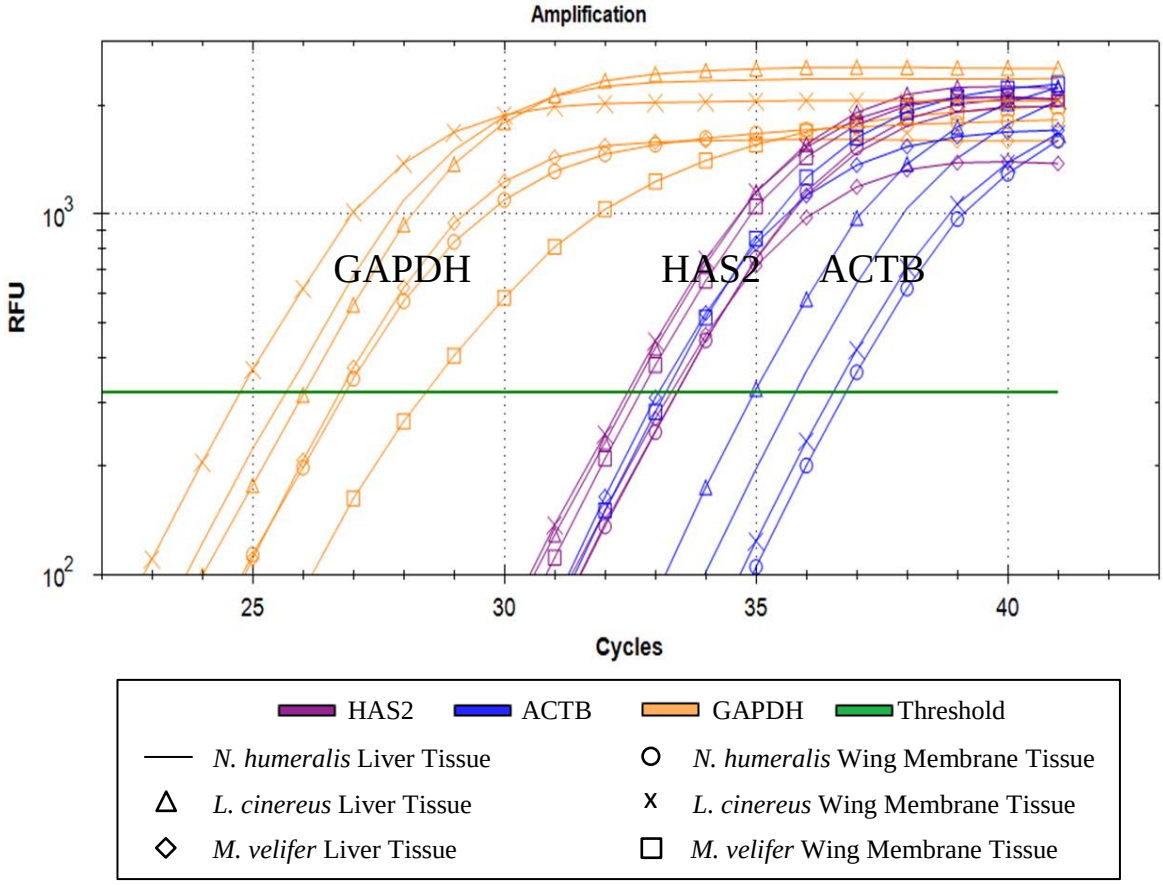

Figure 7. Real-time PCR amplification curve of *N. humeralis, L. cinereus,* and *M. velifer* liver and wing membrane tissue samples with HAS2 primer set. All samples exhibited successful amplification. Primers include HAS2 (purple), GAPDH (orange), and ACTB (blue).

Melt peak analysis (Figure 8) revealed strong peaks for GAPDH at around 86.5ºC, the expected product melting temperature. The peaks for ACTB were between the melting temperatures 76.5ºC and 77.0ºC which follows the trend from the previous trial. This temperature range is the expected melting temperature for the primers, not the product. The peaks for HAS2 are below the set threshold value and some of the samples display two peaks that indicate the presence of an unspecific product. However, the peaks are around the expected product melting temperature of 88.0ºC.

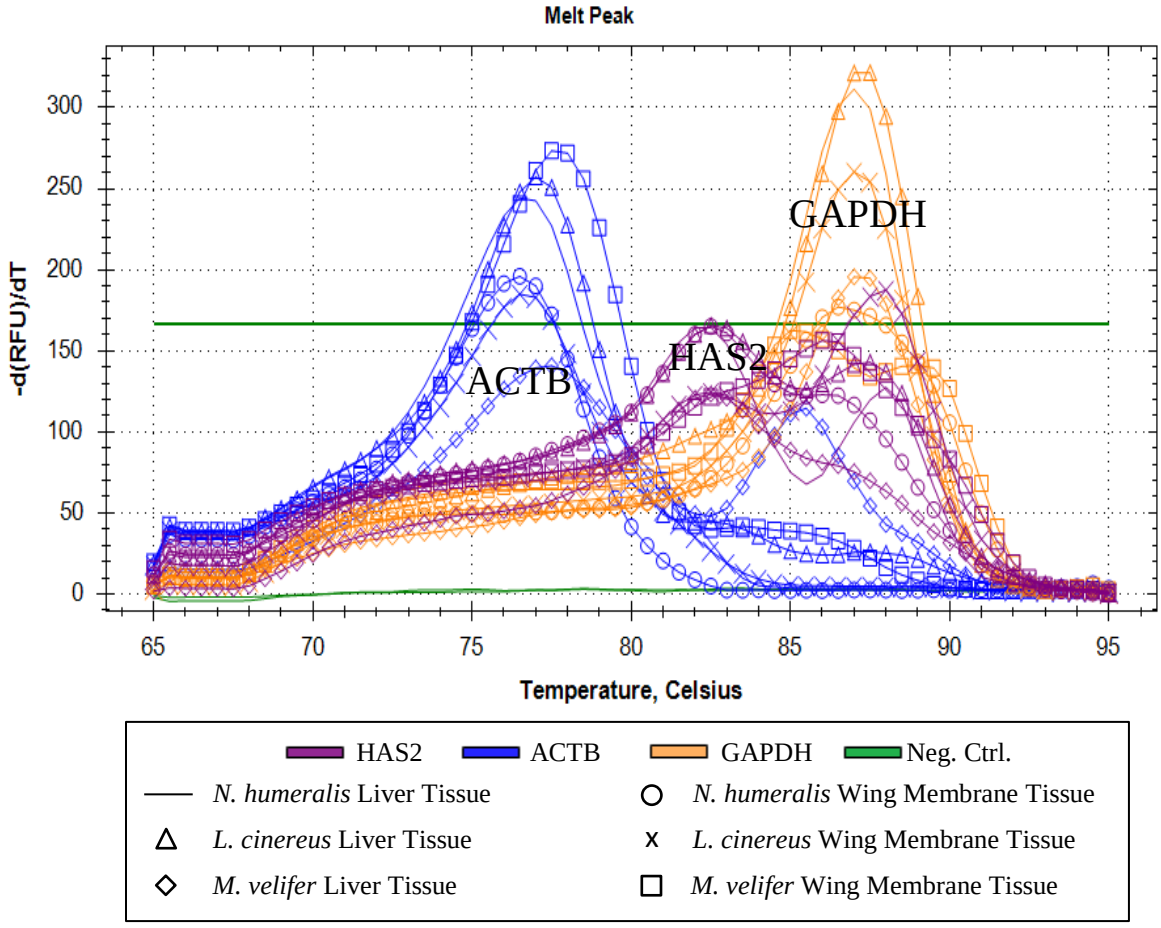

Figure 8. Real-time PCR melt peak analysis of *N. humeralis*, *L. cinereus*, and *M. velifer* liver and wing membrane tissue samples with the HAS2 primer set. Primers include HAS2 (purple), GAPDH (orange), and ACTB (blue). HAS2 melt peaks are below the threshold value and some display two peaks, indicating the presence of unspecific product. Negative control samples are green.

ΔCq gene expression analysis revealed that HAS2 was expressed more in wing membrane tissue samples as compared to the liver tissue samples, except in *M. velifer* (Figure 9). The ΔCq gene expression of HAS2 is higher than the reference genes for samples *L. cinereus* liver tissue (2L), *M. velifer* liver tissue (3L), and *N. humeralis* wing membrane tissue (1W) samples.

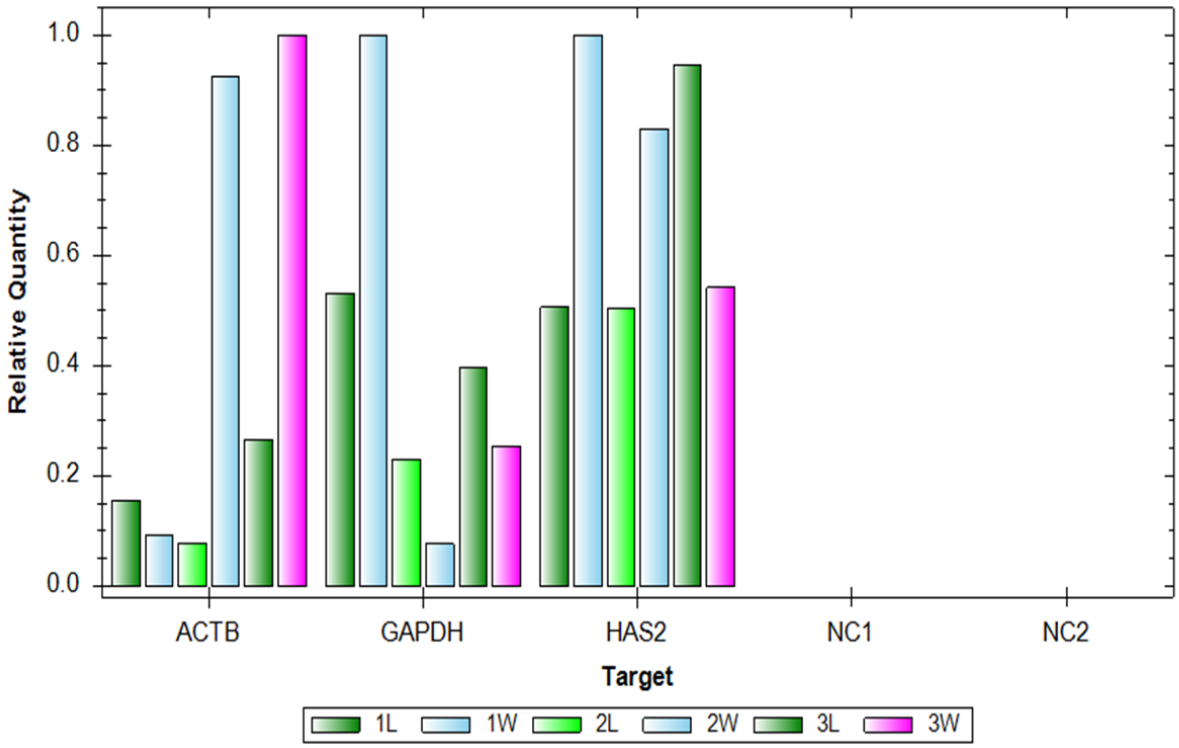

Figure 9. Relative quantity (ΔCq) gene expression of *N. humeralis* (1), *L. cinereus* (2), and *M. velifer* (3) liver (L) and wing membrane (W) tissue samples for HAS2 primer set. Each of the three species is designated by the number 1, 2, or 3, and the liver tissue or wing membrane tissue samples are designated by the letter L or W.

Electrophoresis analysis of the real-time PCR products using a 1.0% agarose gel resulted in moderate banding for HAS2 at around 350 base pairs for *N. humeralis* (Figure 10). Also, there was weak and smeared banding for HAS2 for *L. cinereus and M. velifer*. GAPDH was associated with strong banding at around 400 base pairs for each of the species, and no banding was exhibited for ACTB.

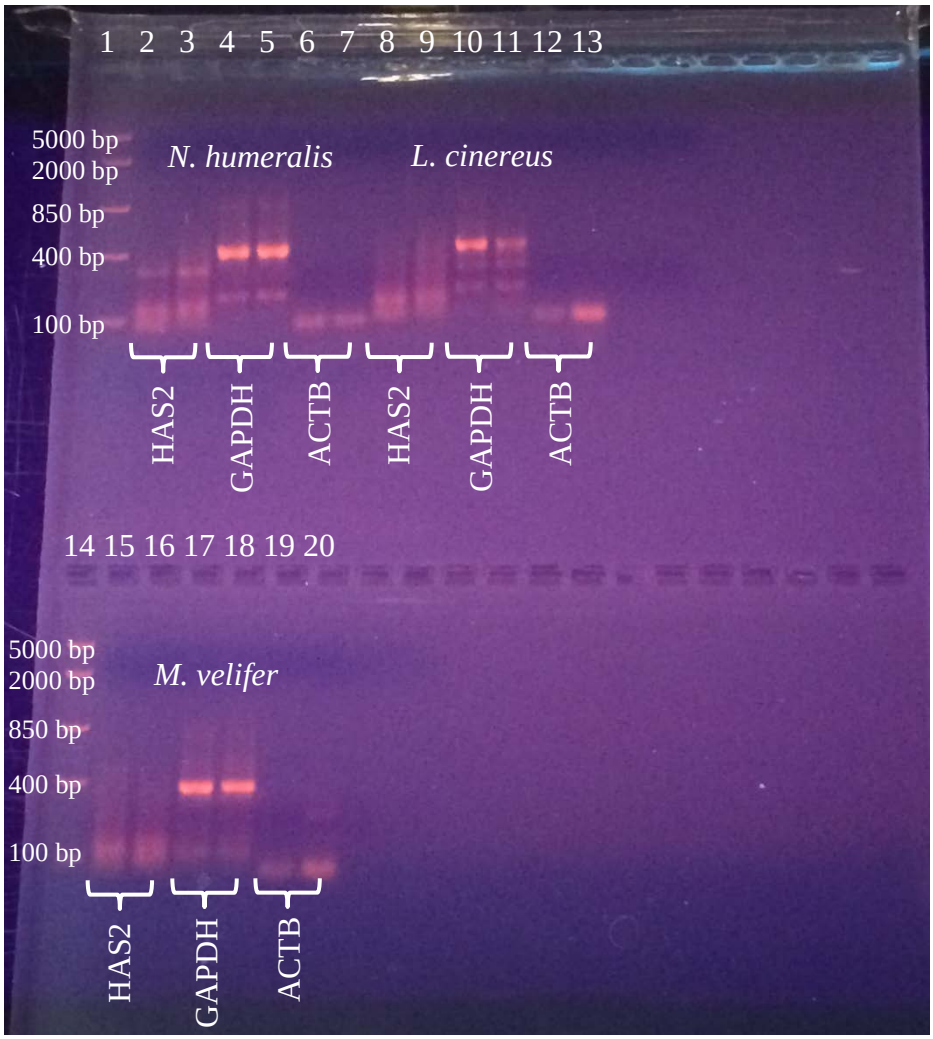

Figure 10. Electrophoresis analysis of *N. humeralis, L. cinereus,* and *M. velifer* liver and wing membrane tissue samples. Samples include HAS2 liver and wing membrane tissue samples for each respective species (lanes 2-3, 8-9, and 15-16), GAPDH liver and wing membrane tissue (lanes 4-5, 10-11, and 17-18), and ACTB liver and wing membrane tissue (lanes 6-7, 12-13, and 19-20). Lane 1 and 14 contain the mid range DNA ladder.

Several succeeding trials were conducted and annealing temperature or starting cDNA template amount were altered in order to improve results. Increasing the annealing temperature from 60°C to 62°C did not result in any significant changes in the results, but lowering the annealing temperature from 60°C to 58°C resulted in no amplification for two of the samples (data not included). Increasing or decreasing the amount of starting cDNA template did not show a substantial change in the output (data not included).

Real-Time PCR Trial 3

After unsuccessful amplification of several samples and unsatisfying melt curve analysis despite changes in the real-time PCR protocol, the cDNA generated from *N. humeralis, L. cinereus, and M. velifer* liver and wing membrane tissue samples were subjected to real-time PCR using HAS2(2), GAPDH, and ACTB primers (Table 1). Quantification data revealed no amplification of *L. cinereus* liver tissue sample with the newly designed HAS2(2) primer, and melt peak analysis showed double peaks and values below the expected threshold for HAS2(2) (data not included). Gene expression analysis could not be completed due to the unsuccessful amplification of the *L. cinereus* liver tissue sample with the HAS2(2) primer pair. No electrophoresis analysis was completed.

Real-Time PCR Trial 4 and Real-Time PCR Gene Study

The cDNA generated from *N. humeralis*, *L. cinereus*, and *M. velifer* liver and wing membrane tissue samples were subjected to real-time PCR using the HAS2(1), GAPDH, and ACTB primers (Table 1). Results revealed that each sample successfully showed amplification without any of the negative controls amplifying (Figure 11). GAPDH amplified first between cycles 22 and 25, followed by HAS2(1) between cycles 27 and 31. ACTB amplified last between cycles 29 and 32.

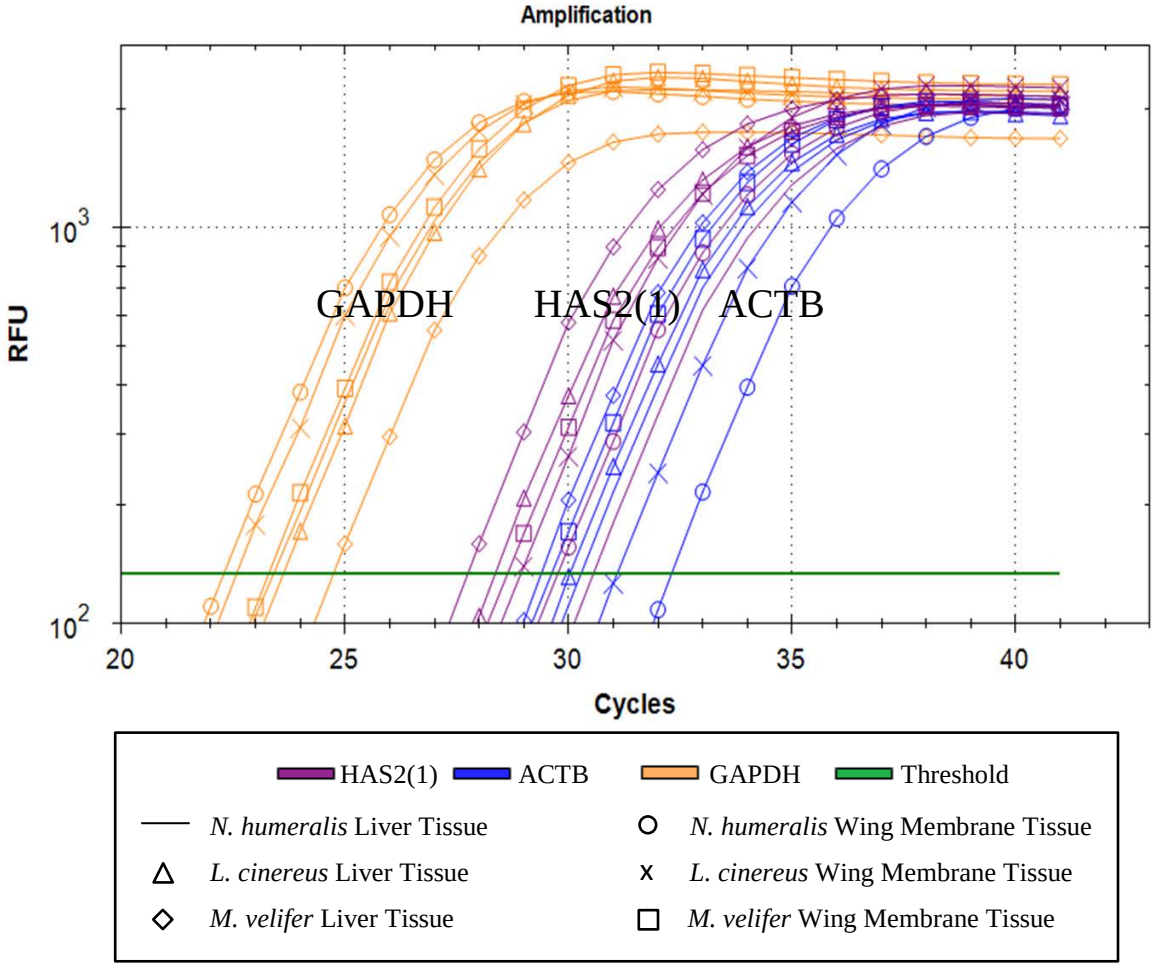

Figure 11. Real-time PCR amplification curve of *N. humeralis*, *L. cinereus*, and *M. velifer* liver and wing membrane tissue samples with HAS2(1) primer set. All samples exhibited successful amplification. Primers include HAS2(1) (purple), GAPDH (orange), and ACTB (blue).

Melt peak analysis (Figure 12) revealed strong peaks for GAPDH at around 86.5ºC, the expected product melting temperature. The peaks for ACTB were between the melting temperatures 76ºC and 78.0ºC which follows the trend from the previous trials. The peaks for HAS2 were also strong between the melting temperatures 76ºC and 78.0ºC, indicating primer amplification.

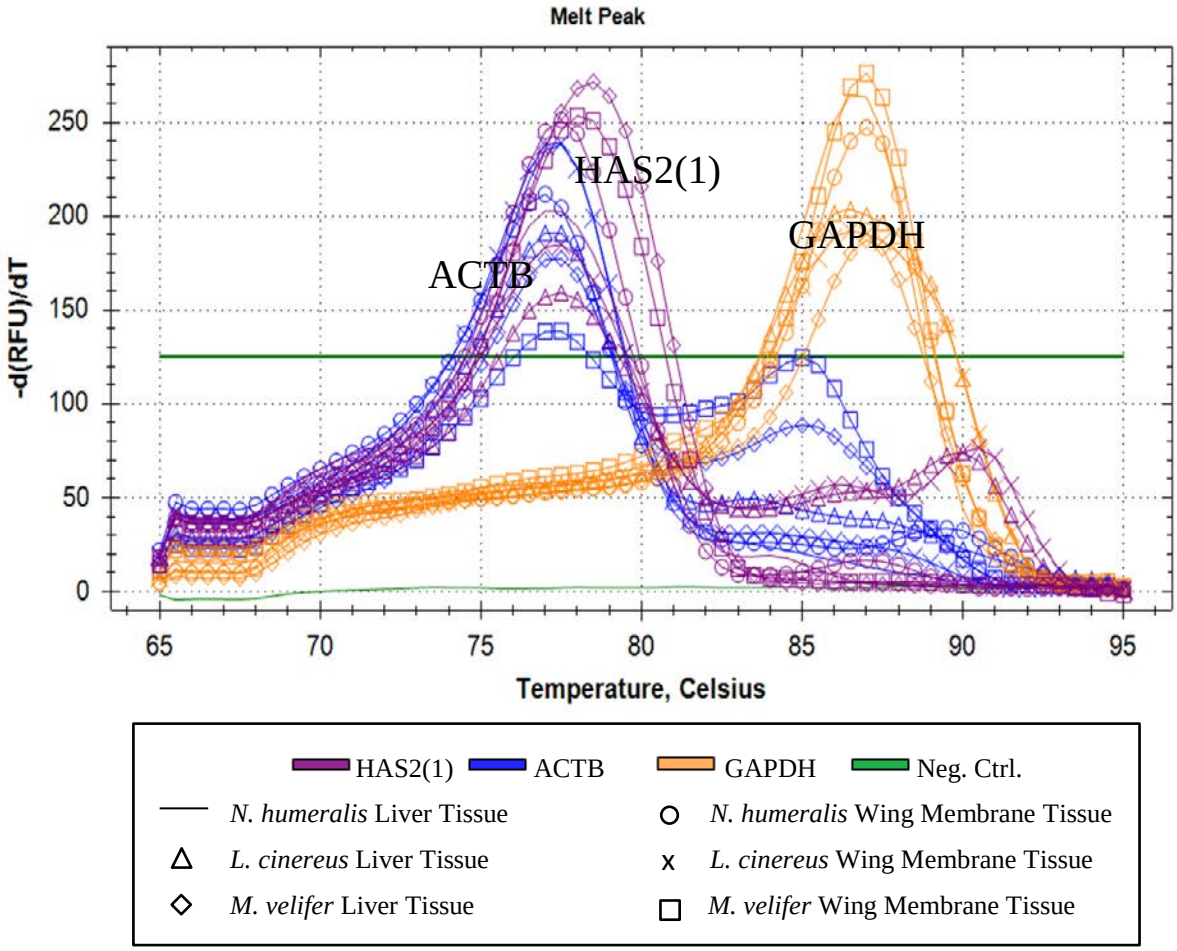

Figure 12. Real-time PCR melt peak analysis of *N. humeralis* (1), *L. cinereus* (2), and *M. velifer* (3) liver (L) and wing membrane (W) tissue samples with HAS2(1) primer set. Primers include HAS2(1) (purple), GAPDH (orange), and ACTB (blue). Negative control samples are green.

ΔCq gene expression analysis revealed that HAS2 was expressed more in wing membrane tissue samples from *N. humeralis* and *M. velifer* as compared to the liver tissue samples (Figure 13). *L. cinereus* had higher HAS2 expression in liver tissue sample as compared to the wing membrane tissue sample.

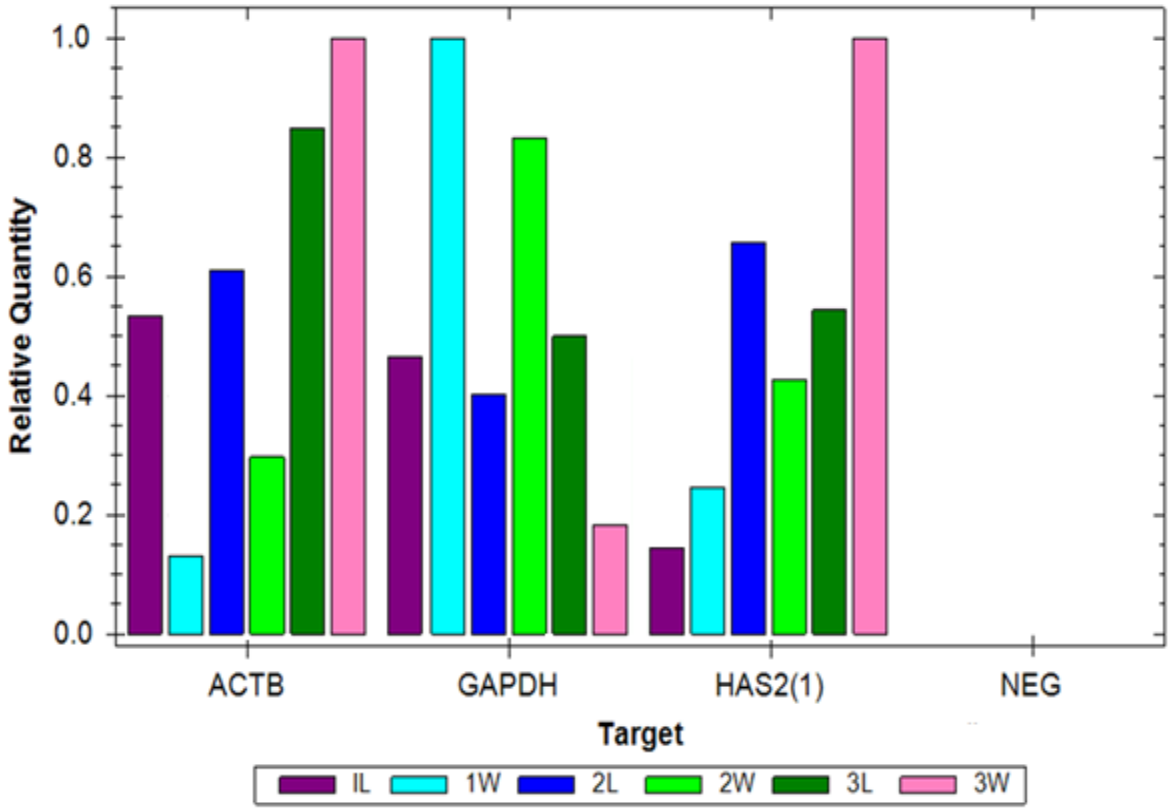

Figure 13. Relative quantity (ΔCq) gene expression of *N. humeralis* (1), *L. cinereus* (2), and *M. velifer* (3) liver (L) and wing membrane (W) tissue samples for HAS2(1) primer set.

This trial was repeated three times in order to construct a gene study that combines data from multiple trials. The reference gene ACTB was removed from the gene study due to unsuccessful amplification in subsequent trials. The normalized gene expression of HAS2 in the gene study was higher in wing membrane tissue samples from each of the three species of bats as compared to the liver tissue samples (Figure 14). The expression levels were normalized to the expression levels of GAPDH in each of the examined tissue samples.

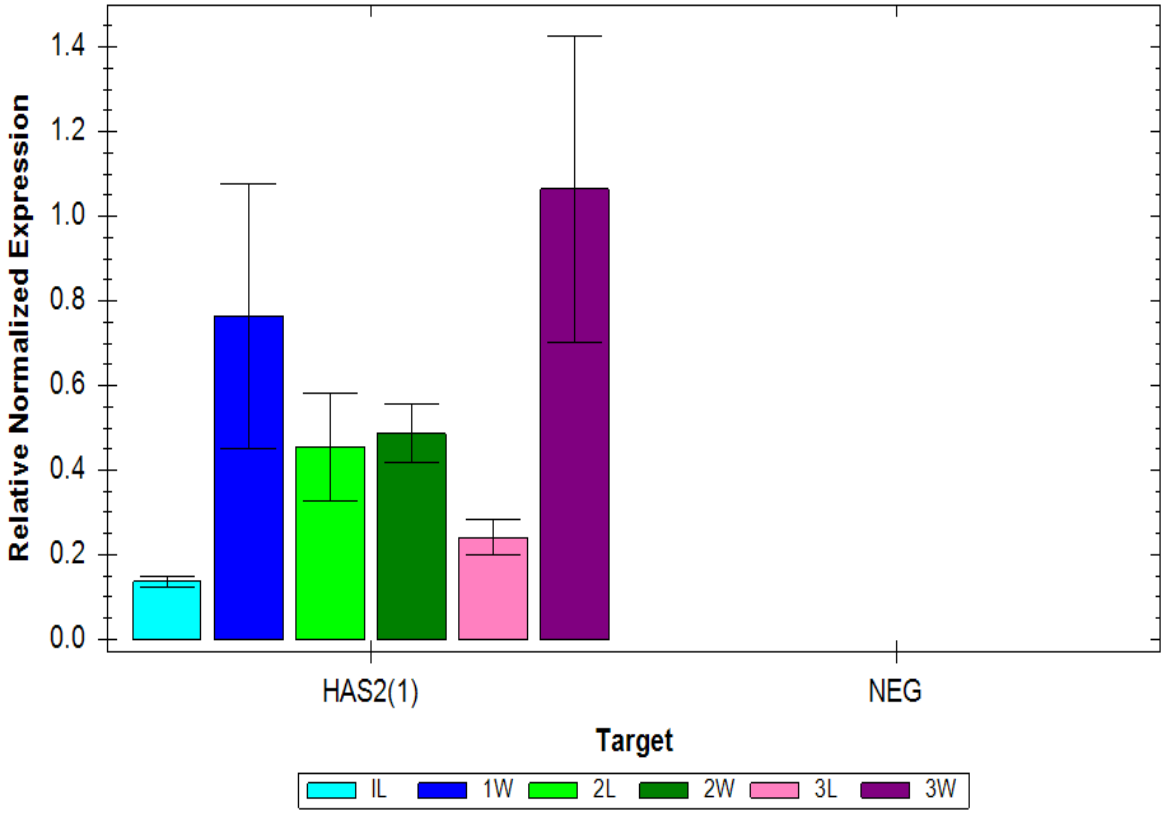

Figure 14. Normalized gene expression of *N. humeralis* (1), *L. cinereus* (2), and *M. velifer* (3) liver (L) and wing membrane (W) tissue samples for 3 trials with the HAS2(1) primer set.

Real-Time PCR from Angelo State University Molecular Biology Class

Students in the Molecular Biology course at Angelo State University completed real-time PCR using cDNA generated from *N. humeralis, L. cinereus,* and *M. velifer* kidney and heart tissue samples. The primers used included ACTB and HAS2(1) (Table 1). In these trials, quantification data revealed that the negative controls for HAS2(1) amplified (Figure 15).

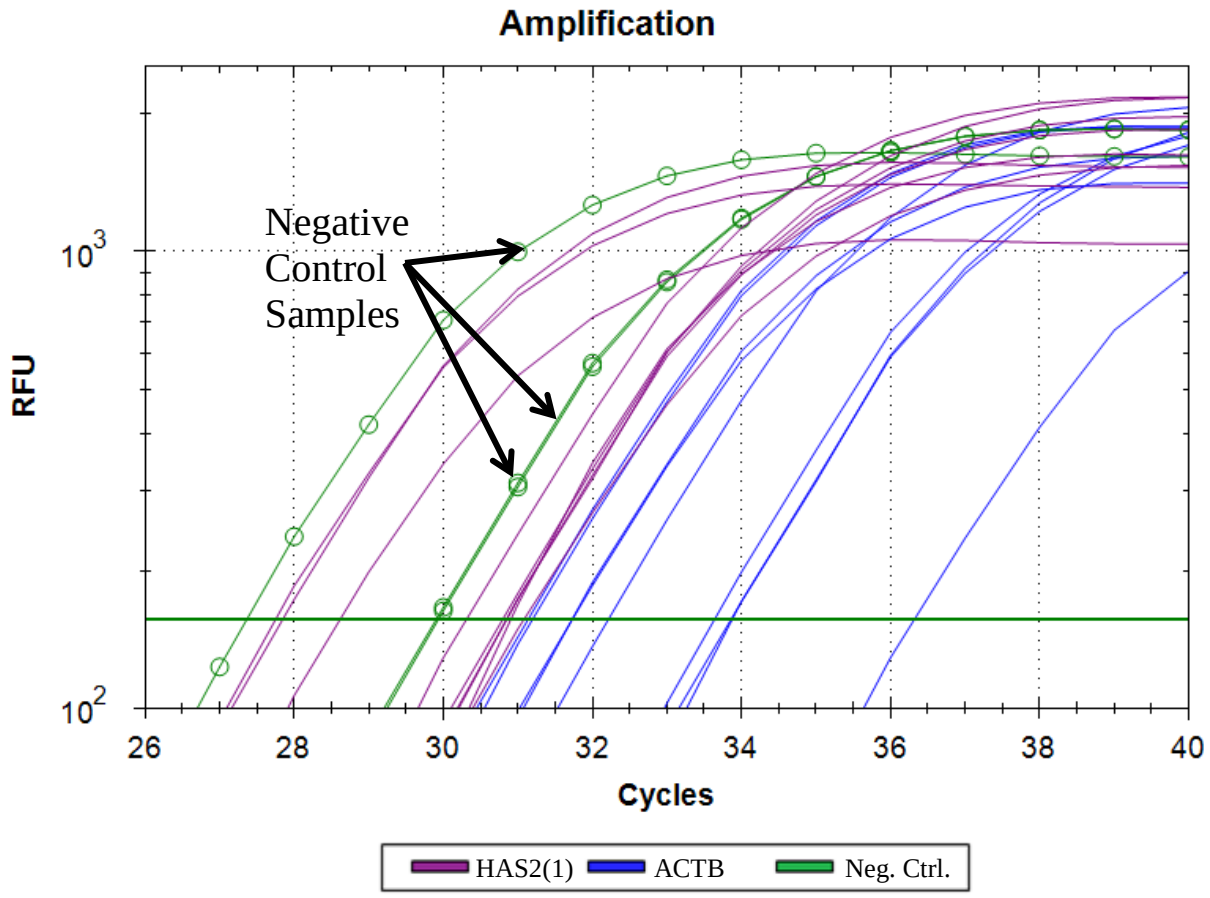

Figure 15. Real-time PCR amplification shows amplification of HAS2(1) negative controls (green lines with circles).

The melt peak analysis revealed that the negative control for HAS2(1) showed a melting peak along with all of the other samples between 76.5ºC and 78.0ºC, which represent the expected melting temperatures for the primers and not the products of the reaction (Figure 16).

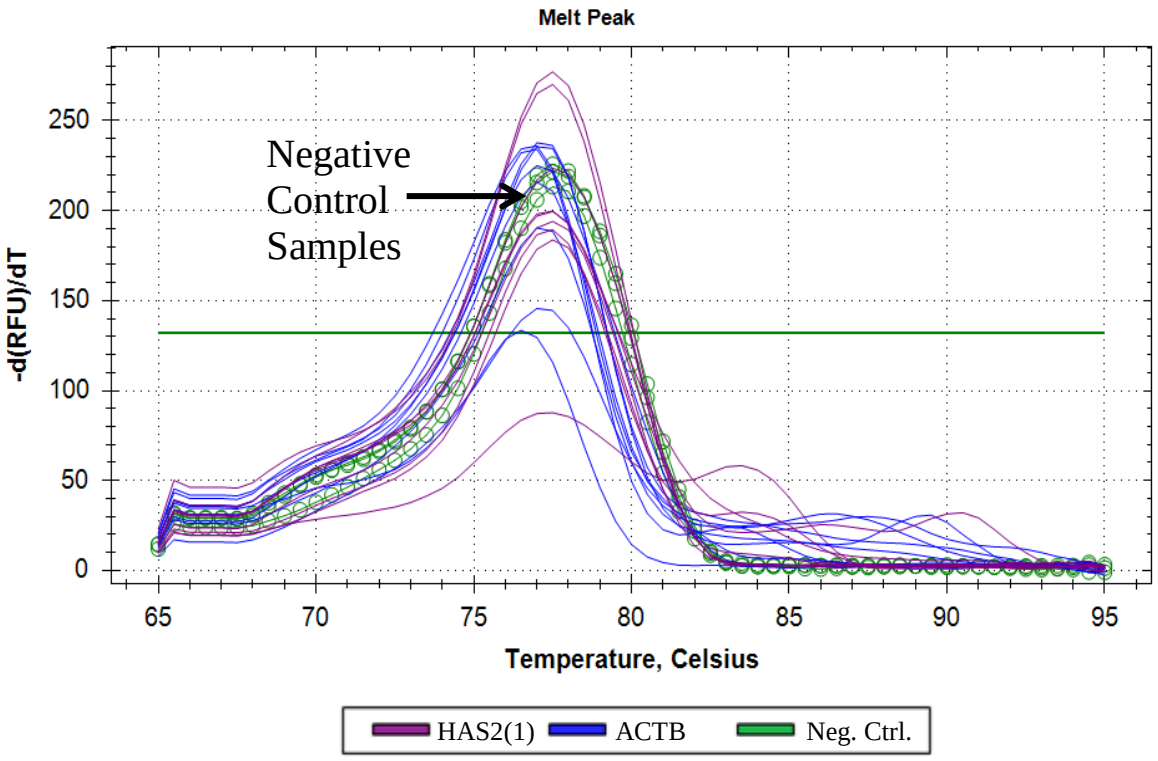

Figure 16. Melt peak analysis indicates the presence of primer dimer with the HAS2(1) negative control melt peak (green lines with circles)

Gene expression analysis could not be completed because the negative control for HAS2(1) showed amplification. Electrophoresis analysis using a 1.0% agarose gel revealed that none of the samples produced a product because there was no banding (photo not shown).

Conventional PCR of cDNA

Conventional PCR of cDNA from *N. humeralis* liver and wing membrane tissue samples with GAPDH and the primers HAS2(3), HAS2(4), HAS2(5), HAS2(6), and HAS2(7) resulted in positive banding only for samples with the GAPDH primers (data not included). In addition, conventional PCR of cDNA from house mouse liver and skin tissue samples with GAPDH and all HAS2 primers resulted in faint, smeared banding for the primers HAS2 and HAS(4) (Figure 17). There was no banding associated for any of the other HAS2 primer sets or for the reference gene GAPDH.

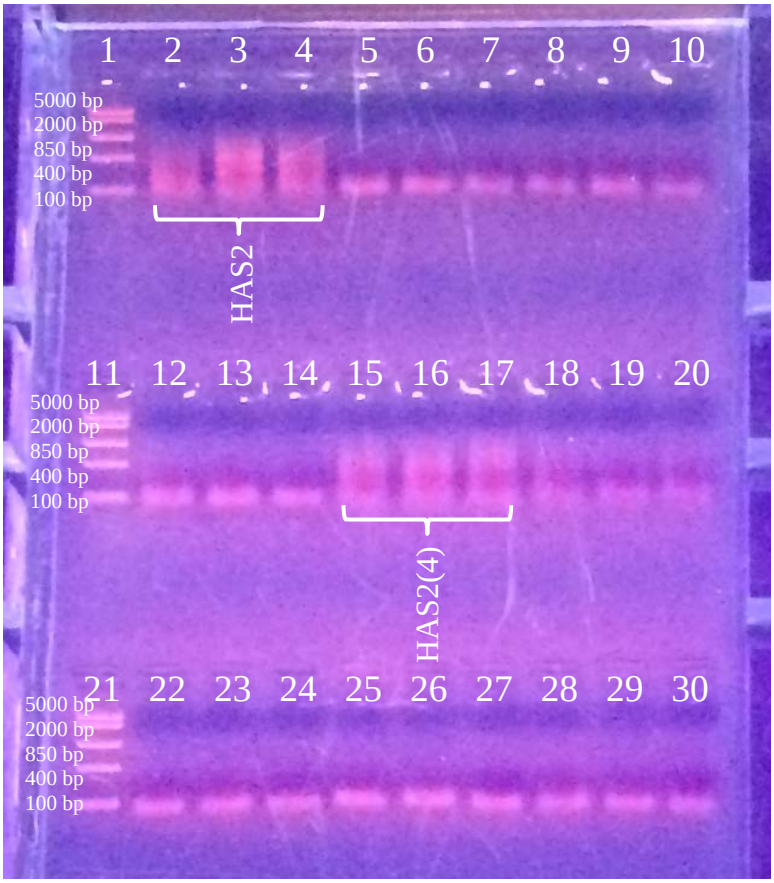

Figure 17. Electrophoresis analysis of house mouse liver and skin tissue samples with newly purchased HAS2 primer sets. Primers HAS2 (lanes 2-4) and HAS2(4) (lanes 15-17) showed smeared banding for liver, skin, and negative control samples. Lanes 1, 11, and 21 contain the mid range DNA ladder.

DNA Extraction and Conventional PCR

The concentration of DNA extraction from mouse, naked mole rat, Damaraland mole rat, hoary bat, and cave myotis liver tissue samples was determined using the NanoDrop Lite Spectrophotometer (Table 4). As expected, the first elution of each tissue sample resulted in a higher concentration of DNA as compared to the second elution, except for the *H. glaber* liver sample. The purity ratio of the DNA for each of the tissue samples examined was between 1.56 and 2.04, so some of the sample fall below or above the desired range of around 1.80.

Table 4. Amount of genomic DNA extracted from liver of mouse, naked mole rat, Damaraland mole rat, hoary bat, and cave myotis.

Sample	Elution #	Purity Ratio	Concentration (µg/ml)
M. musculus Liver	1	2.03	893.9
M. musculus Liver	2	2.02	359.2
H. glaber Liver	1	1.66	160.8
H. glaber Liver	2	1.56	251.0
F. damarensis Liver	1	1.61	479.0
F. damarensis Liver	2	1.60	209.2
L. cinereus Liver	1	2.01	572.3
L. cinereus Liver	2	2.04	210.9
M. velifer Liver	1	1.85	247.0
M. velifer Liver	2	1.89	110.0

All primers, including the reference genes ACTB and GAPDH, were used in a conventional PCR using the extracted DNA as the template to determine which primers exhibited positive or negative amplification of HAS2. The primers HAS2 and HAS2(2) showed positive banding and no banding of the negative control samples (Figure 18). In addition, ACTB showed faint banding and GAPDH showed slightly stronger banding. The primers HAS2(3) and HAS2(4) showed banding, but the negative controls containing just primer also showed banding.

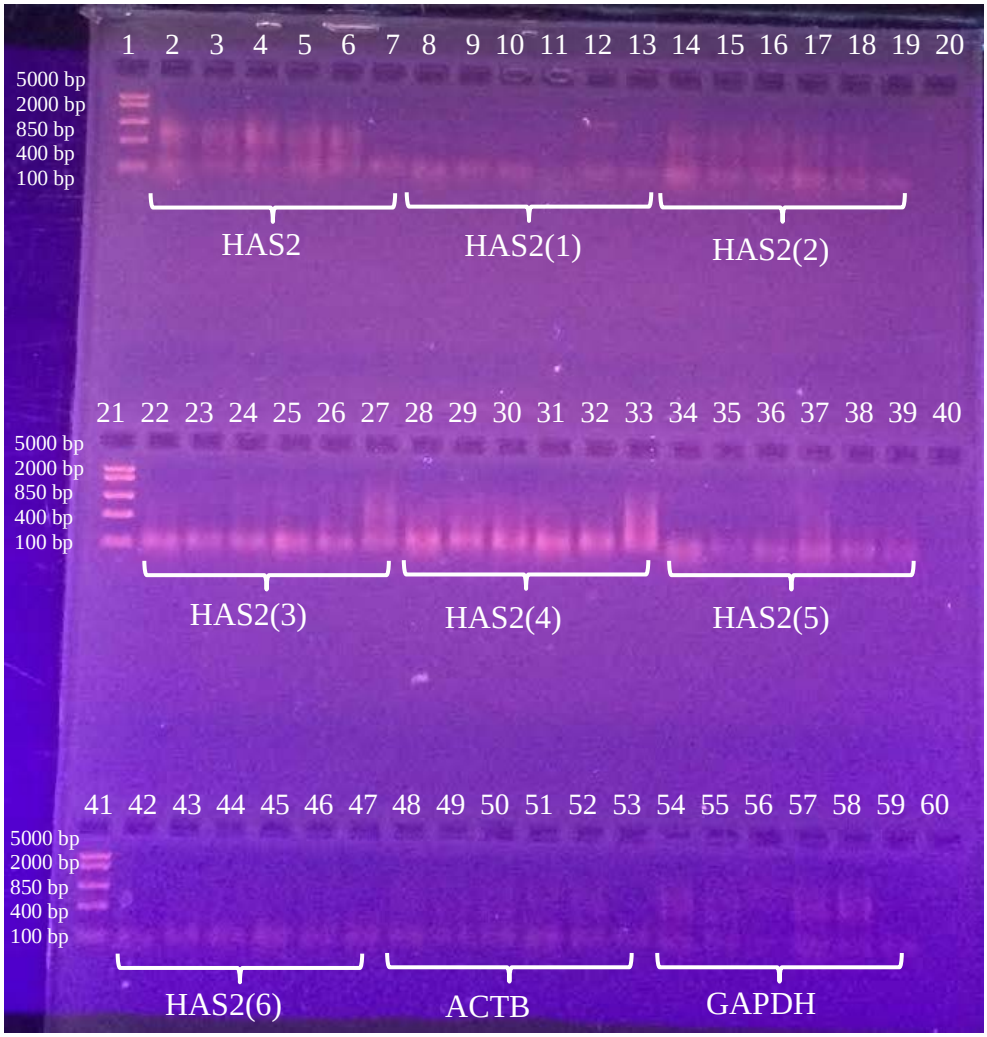

Figure 18. Electrophoresis analysis of primers tested with extracted DNA from liver tissue samples. Primers HAS2 (lanes 2-7) and HAS2(2) (lanes 14-19) showed banding for HAS2.

DISCUSSION

Examination of the sequence alignments revealed that all bat species studied did not contain the unique amino acid substitutions in HAS2 that the naked mole rat possesses, as described by Tian et al. (2013). However, it was revealed that the Damaraland mole rat contained the same unique sequence of HAS2 as the naked mole rat at site 301. The Damaraland mole rat is a close relative of the naked mole rat, and the species serves as an additional model organism for longevity research due to the recently sequenced genome (Fang et al., 2014). Further investigation into the shared characteristics between naked mole rats and Damaraland mole rats might shed light on common longevity mechanisms in the two species. In contrast to the shared characteristic between the naked mole rat and Damaraland mole rat, the blind mole rat (*Nannospalax galili),* another long-lived rodent, did not contain the unique HAS2 protein sequence. These results are paralleled with a recently published article regarding the evolution of the HAS2 gene in mammals. In the study, it was found that the unique substitution at site 301 was shared by all African mole rats and the substitution at site 178 was only unique to the naked mole rat and one other mammal, the cane rat, which is an outgroup to the African mole rat group (Faulkes et al., 2015). The polymorphism at site 301 is consistent with the data presented in my study, and the HAS2 protein sequences from the other African mole rat species examined were not available during my data collection.

Real-time PCR trials using multiple published primers designed to be specific for the HAS2 region resulted in inconclusive data. In addition, results were inconclusive despite additional efforts to design primers specific for the HAS2 region for each of the species examined. Therefore, gene expression analysis conclusions cannot be made until HAS2 primers are successfully generated to isolate the HAS2 gene. Results from real-time PCR

trials 1 and 2 revealed that the HAS2 primer set (Tien et al., 2013) resulted in amplification of the desired product, but melt peak analysis showed two peaks during each trial. This suggests that unspecific products were also being amplified, such as hybridized primers, commonly known as primer dimer. Despite changing cycling conditions and cDNA template amounts, the melt peak analysis continued to indicate the amplification of unspecific products. In addition, the reference gene ACTB appeared to show correct quantification and melt peak analysis throughout the trials. However, electrophoresis analysis resulted in no banding for ACTB, indicating that the displayed quantification was primer dimer instead of amplified HAS2 regions from the cDNA template. The hybridized primers were amplifying as the reaction progressed, resulting in a false positive outlook during the gene expression analysis. Throughout the trials, the reference gene GAPDH showed conclusive amplification, promising melt peak data, and positive banding during electrophoresis analysis. The fact that GAPDH showed conclusive results throughout the trial indicates that there is cDNA present for each sample tested. This indicates that the absence of proper amplification for HAS2 and ACTB is due to unspecific primer design, not a lack of cDNA present.

After the unsuccessful trials with the HAS2 primer set, the primers HAS2(1) and HAS2(2) were designed and ordered with the hopes of obtaining successful amplification of the HAS2 gene region without amplification of unspecific products. Real-time PCR trial with the HAS(2) primer resulted in unsuccessful amplification of certain samples and unsatisfactory melt peak data, indicating that the primer was not binding to the desired HAS2 region on the cDNA template strands. Real-time PCR trial 4 with the HAS2(1) primer resulted in what appeared to be successful amplification for each of the samples. Melt peak analysis did not contain double peaks as previously seen in earlier trials. However, the melt

peaks for HAS2(1) and ACTB were between the melting temperatures 76.5ºC and 78.0ºC, which were the expected melting temperatures for the primers, not the product. This unfortunate result was not recognized and understood before moving on to subsequent trials and the comprehensive gene study. Data from the gene study cannot be used to determine the expression level of HAS2 within the bat species examined due to the fact that all quantification data involving the primer HAS2(1) probably was primer dimer, not the HAS2 gene region amplifying.

Data from the Molecular Biology class at Angelo State University clearly confirmed the ineffective nature of the primers HAS2(1) and ACTB. Real-time PCR data resulted in amplification of all HAS2(1) negative control samples, indicating that primer dimer was occurring. The melt peak for both HAS2(1) and ACTB fell at the lower temperature, and the negative control samples each displayed a melt peak. This further indicates that the quantification shown in trial 4, the subsequent gene study, and the molecular biology trial was a result of primer amplification, not the desired product amplification.

A total of five new primer sets were designed or retrieved from various studies, and each new primer set was tested using conventional PCR. When DNA was extracted from mouse, naked mole rat, Damaraland mole rat, hoary bat, and cave myotis liver tissue samples at the conclusion of the study, conventional PCR revealed that only the HAS2, HAS2(2), GAPDH, and ACTB primers showed faint, but promising banding. This indicates that these primers might be successful in real-time PCR quantification and gene expression analysis in future studies once the protocol is refined.

Several factors could contribute to the inconclusive results obtained from the study. Due to the insufficient quantification in real-time PCR trials and undetectable banding in

electrophoresis analysis, the primers designed or selected for the study might not have been as specific to the samples from each species as they should have been. Primer design serves as one of the most important steps when designing a real-time PCR experiment. It is crucial to ensure that the primers chosen anneal to the desired cDNA regions, do not display self-hybridization, and are used at sufficient concentrations in the experiment (Derveaux et al., 2010). Although HAS2 is noted to be a highly conserved gene region in mammalian species (Spicer and McDonald, 1998), the designed or published primers selected for this study were not effective across all of the species examined.

Another possible contributing factor to the inconclusive results is the concentration of RNA or cDNA used throughout the experiment. The DNA extracted from the liver tissue was at a much higher concentration as compared to the RNA extracted earlier in the study, which could explain the positive results in the conventional PCR reaction. Having a higher starting RNA concentration could produce a larger yield of cDNA during cDNA synthesis. It is very possible that having a low concentration of cDNA template during each of the real-time PCR trials could have strongly contributed to the unsuccessful quantification of the desired HAS2 gene region. In addition, the extracted RNA or synthesized cDNA could have degraded throughout the duration of the study. This could result in even lower concentrations of starting template for each of the real-time PCR trials.

Several future directions of this study could be explored to determine if bats utilize the same molecular mechanism present in naked mole rats. Sequencing the DNA extracted from the liver tissue samples of mouse, naked mole rat, Damaraland mole rat, hoary bat, and cave myotis will be a valuable step. Once the sequence is retrieved, it can be aligned and used to determine possible primers specific to the samples being used. The expression levels

of HAS2 could then be determined and successful gene expression analysis could be performed. In addition, because the Damaraland mole rat was shown to have the same unique HAS2 protein sequence as the naked mole rat, investigation into the expression levels of HAS2 in Damaraland mole rats could unlock another longevity mechanism present within the species. Although this step would not involve bats, this information could contribute to the study of aging.

In conclusion, although none of the examined bat species contained the same unique HAS2 protein sequence displayed by the two mole rats, it is still possible that the mechanism involving HAS2 plays a role in longevity within certain species of bats. Organismal cellular mechanisms are very complex and can be influenced by a multitude of factors. This is especially true with the large group of extremely diverse bat species that live in highly variable environments across the globe. Understanding the mechanisms involving longevity in bat species, as well as other long-lived organisms, has significant value within the scientific community. The complex processes that occur in these species could be used to improve the lives of many individuals by unlocking the mysteries of age-related diseases, such as neurodegenerative disorders and cancer. Therefore, continued research with bats, naked mole rats, and other long-lived species is extremely valuable and has the potential to significantly add to our understanding of aging.

LITERATURE CITED

Adams, R.A., and Pedersen, S.C. (2000). Ontogeny, Functional Ecology, and Evolution of Bats (London; New York: Cambridge University Press).

Altringham, J.D. (2011). Bats: from evolution to conservation (New York: Oxford University Press).

Austad, S.N., and Fischer, K.E. (1991). Mammalian aging, metabolism, and ecology: evidence from the bats and marsupials. J. Gerontol. *46*(2), B47-B53.

Bennett, N.C., and Faulkes, C.G. (2000). African Mole-Rats: Ecology and Eusociality (Cambridge, U.K.: Cambridge University Press).

Buffenstein, R. (2008). Negligible senescence in the longest living rodent, the naked mole-rat: insights from a successfully aging species. J. Comp. Physiol. B Biochem. Syst. Environ. Physiol. *178*, 439-445.

Chen, W., and Abatangelo, G. (1999). Functions of hyaluronan in wound repair. Wound Repair Regen. *7*(2), 79-89.

Chun-E, R., Xueqiong, Z., Jinping, L., Lyle, C., Dowdy, S., Podratz, K.C., Byck, D., Hai-Bin, C., Shi-Wen, J. (2015). Microarray Analysis on Gene Regulation by Estrogen, Progesterone and Tamoxifen in Human Endometrial Stromal Cells. Int. J. Mol. Sci. *16*(3), 5864-5885.

Derveaux, S., Vandesompele, J., and Hellemans, J. (2010). How to do successful gene expression analysis using real-time PCR. Methods *50*(4), 227-230.

Edrey, Y.H., Hanes, M., Pinto, M., Mele, J., and Buffenstein, R. (2011). Successful aging and sustained good health in the naked mole rat: a long-lived mammalian model for biogerontology and biomedical research. ILAR J. *51*(1), 41-53.

Fang, X., Seim, I., Huang, Z., Gerashchenko, M.V., Xiong, Z., Turanov, A.A., Zhu, Y., Lobanov, A.V., Fan, D., Yim, S.H., et al. (2014). Adaptations to a subterranean environment and longevity revealed by the analysis of mole rat genomes. Cell Rep. *8*(5), 1354-1364.

Faulkes, C.G., Davies, K.T., Rossiter, S.J., and Bennett, N.C. (2015). Molecular evolution of the hyaluronan synthase 2 gene in mammals: implications for adaptations to the subterranean niche and cancer resistance. Biol. Lett. *11*(5), 20150185.

Fenton, M.B. (2001). Bats (New York, NY: Checkmark Books).

Fraser, J.R., Laurent, T.C., and Laurent, U.B. (1997). Hyaluronan: its nature, distribution, functions and turnover. J. Intern. Med. *242*(1), 27-33.

Hayssen, V., and Kunz, T.H. (1996). Allometry of litter mass in bats: maternal size, wing morphology, and phylogeny. J. Mammal. *77*(2), 476-490.

Healy, K., Guillerme, T., Finlay, S., Kane, A., Kelly, S. B., McClean, D., Kelly, D.J., Donohue, I., Jackson, A.L., Cooper, N. (2014). Ecology and mode-of-life explain lifespan variation in birds and mammals. P. Roy. Soc. Lond. B Bio. *281*(1784), 20140298.

Jenkins, R.H., Thomas , G.J., Williams , J.D., and Steadman, R. (2004). Myofibroblastic differentiation leads to hyaluronan accumulation through reduced hyaluronan turnover. J. Biol. Chem. *279*(40), 41453-41460.

Karbownik, M. S., and Nowak, J. Z. (2013). Hyaluronan: Towards novel anti-cancer therapeutics. Pharmacol. Rep. *65*(5), 1056-1074.

Kothapalli, D., Flowers, J., Xu, T., Pure, E., and Assoian, R.K. (2008). Differential activation of ERK and Rac mediates the proliferative and anti-proliferative effects of hyaluronan and CD44. J. Biol. Chem. *283*(46), 31823-31829.

Kothapalli, D., Zhao, L., Hawthorne, E. A., Cheng, Y., Lee, E., Pure, E., and Assoian, R.K. (2007). Hyaluronan and CD44 antagonize mitogen-dependent cyclin D1 expression in mesenchymal cells. J. Cell Biol. *176*(4), 535-544.

Kunz, T.H. (1982). Ecology of bats (New York: Plenum Press).

Kunz, T.H., and Fenton, M.B. (2003). Bat ecology (Chicago: University of Chicago Press).

Lewis, K.N., Andziak, B., Yang, T., and Buffenstein, R. (2013). The naked mole-rat response to oxidative stress: just deal with it. Antioxid. Redox Signal. *19*(12), 1388-1399.

Lewis, S.E. (1995). Roost Fidelity of Bats: A Review. J. Mammal. *2*, 481-496.

Podlutsky, A.J., Khritankov, A.M., Ovodov , N.D., and Austad, S.N. (2005). A new field record for bat longevity. J. Gerontol. A Biol. Sci. Med. Sci. *60*(11), 1366-1368.

Pure, E., and Assoian, R.K. (2009). Rheostatic signaling by CD44 and hyaluronan. Cell. Signal. *21*(5), 651-655.

Redfern, R.L., Reins, R.Y., and McDermott, A.M. (2011). Toll-like receptor activation modulates antimicrobial peptide expression by ocular surface cells. Exp. Eye Res. *92*, 209-220.

Seluanov, A., Hine, C., Azpurua , J., Feigenson, M., Bozzella, M., Mao, Z., Catania, K.C., and Gorbunova, V. (2009). Hypersensitivity to contact inhibition provides a clue to cancer resistance of naked mole-rat. Proc. Natl. Acad. Sci. U.S.A. *106*(46), 19352-19357.

Spicer, A., and McDonald, J. (1998). Characterization and molecular evolution of a vertebrate hyaluronan synthase gene family. J. Biol. Chem. *273*(4), 1923-1932.

Sugiyama, Y., Shimanda, A., Sayo, T., Sakai, S., and Inoue, S. (1998). Putative hyaluronan synthase mRNA are expressed in mouse skin and TGF-β upregulates their expression in cultured human skin cells. J. Invest. Dermatol. *110*(2), 110.

Tamura, K., Stecher, G., Peterson, D., Filipski, A., and Kumar, S. (2013). MEGA6: Molecular Evolutionary Genetics Analysis version 6.0. Mol. Biol. Evol. *30*, 2725-2729.

Tian, X., Azpurua, J., Hine, C., Vaidya, A., Myakishev-Rempel, M., Ablaeva, J., Mao, Z., Nevo, E., Gorbunova, V., and Seluanov, A. (2013). High-molecular-mass hyaluronan mediates the cancer resistance of the naked mole rat. Nature *499*(7458), 346-349.

Tian, X., Azpurua, J., Ke, Z., Augereau, A., Zhang, Z.D., Vijg, J., Gladyshev, V.N., Gorbunova, V., and Seluanov, A. (2015). INK4 locus of the tumor-resistant rodent,

the naked mole rat, expresses a functional p15/p16 hybrid isoform. Proc. Natl. Acad. Sci. U.S.A. *112*(4), 1053-1058.

Tolg, C., Telmer, P., and Turley, E. (2014). Specific sizes of hyaluronan oligosaccharides stimulate fibroblast migration and excisional wound repair. Plos ONE *9*(2), e88479.

Wilkinson, G.S., and South, J.M. (2002). Life history, ecology and longevity in bats. Aging Cell *1*(2), 124-131.

Zhang, G. (2013). Comparative analysis of bat genomes provides insight into the evolution of flight and immunity. Science *339(6118),* 456-459.

Zhu, X., Deng, X., Huang, G., Wang, J., Yang, J., Chen, S., Ma, X., and Wang, B. (2014). A novel mutation of hyaluronan synthase 2 gene in Chinese children with ventricular septal defect. Plos ONE *9*(2), e87437.

VITA

Aimee Nicole Denham was raised in Bandera, Texas, by her two loving and supportive parents, Jacqueline Innanen and Richard Denham, along with her younger sister, Allie Denham. Aimee graduated from Angelo State University in May 2015 with a Bachelor of Science in biology with a chemistry minor and Highest University Honors. Awarded the 2015 Presidential Award as the top graduate of her class, Aimee was an active member in the Honors Program, Honors Student Association, Tri-Beta Biological Honors Society, Joint Admission Medical Program, Alpha Chi, Phi Kappa Phi, and the Women's Track and Field team for a portion of her undergraduate career. She presented this research at the Texas Undergraduate Research Day in Austin, Texas, and the Texas Society of Mammalogists Scientific Meeting in Junction, Texas.

Aimee served as an Honors Student Association officer for three consecutive years, first as Historian for two years and then Vice President. Additionally, she served as an Honors Program mentor and emissary. Aimee received the Director's Award as the outstanding student in the Honors Program. She presented two Student Interdisciplinary Research Panel papers, a research poster, and multiple panel presentation at National Collegiate Honors Council conferences. Additionally, she presented paper, poster, and panel sessions at several Great Plains Honors Council conferences. She served as a voting board member for Galilee Community Development Corporation and the Concho Valley Rape Crisis Center. Following graduation, Aimee will attend Texas Tech University Health Sciences Center School of Medicine in Lubbock, Texas to begin her training toward becoming a physician in the great state of Texas.

Aimee Denham can be contacted via email at adenham@angelo.edu